LICENCE TO McMASTER UNIVERSITY

This Thesis has been written
[Thesis, Project Report, etc.]

by Christopher Martin for
[Full Name(s)]

Undergraduate course number 4K06 at McMaster University under the supervision/direction of Dr. A.P. Dickin.

In the interest of furthering teaching and research, I/we hereby grant to McMaster University:

1. The ownership of 5 copy(ies) of this work;
2. A non-exclusive licence to make copies of this work, (or any part thereof) the copyright of which is vested in me/us, for the full term of the copyright, or for so long as may be legally permitted. Such copies shall only be made in response to a written request from the Library or any University or similar institution.

I/we further acknowledge that this work (or a surrogate copy thereof) may be consulted without restriction by any interested person.

A.P. Dickin
Signature of Witness, Supervisor

Chris Martin
Signature of Student

Sept 8/92
date

MID-PROTEROZOIC EVOLUTION OF THE GRENVILLE BELT: EVIDENCE FROM NEODYMIUM ISOTOPIC MAPPING, BANCROFT, ONTARIO

MID-PROTEROZOIC EVOLUTION OF THE GRENVILLE BELT: EVIDENCE FROM NEODYMIUM ISOTOPIC MAPPING, BANCROFT, ONTARIO

by

Christopher Martin

A Thesis

Submitted to the Department of Geology

in Partial Fulfilment of the Requirements

for the Degree

Honours Bachelor of Science

McMaster University

April, 1992

Honours B.Sc., 4K06 Thesis, 1992

McMaster University

Hamilton, Ontario

TITLE: Mid-Proterozoic Evolution of the Grenville Belt: Evidence from Neodymium Isotopic Mapping, Bancroft, Ontario

AUTHOR: Christopher Martin

SUPERVISOR: Professor A. P. Dickin

NUMBER OF PAGES: 75

Abstract

Detailed Neodymium isotopic mapping was performed on grey gneisses from the Algonquin Park area of Ontario, in the Central Gneiss Belt of the southwestern Grenville Province. The Neodymium model ages determined were based upon the Depleted Mantle Model of DePaolo (1981c). The use of this model is supported by Lead-Lead dating of zircons obtained from an orthogneissic sample.

The wide range of model ages found (1.5 - 1.86 Ga) is attributed to the presence of a northwestward dipping, Andean style, ensialic continental margin arc that was active in the Mid-Proterozoic between 1.50 Ga and 1.65 Ga. The diapiric rise of plutons produced by the subduction zone intruded continental margin at least as old as 1.86 Ga as indicated by the oldest pluton in the field area. Variable amounts of mixing occurred between these orogenic rocks and the existing crustal rocks as illustrated by the variable Neodymium model ages determined for grey gneisses collected between 10 Km and 60 Km north of the Central Metasedimentary Belt Boundary Zone. Major element analysis and subsequent tectonic and petrographic discrimination diagrams such as the AFM plot and the granitoid discrimination diagram of LeFort and Debon (1983) also indicate that the rocks in the Algonquin Park area are calc-alkaline, and are similar to the Peruvian

Coastal Batholith.

For grey gneisses analyzed within 10 Km of the Central Metasedimentary Belt Boundary Zone, the range of ages is far more restricted, suggesting that an island arc approximately 1.45 Ga was transported by the subducting slab and later sutured onto the existing continental margin.

ACKNOWLEDGEMENTS

I wish to thank my supervisor, Dr. Alan P. Dickin for suggesting this research project. I would also like to thank Catharina Jaeger for help in the clean lab and for laughing at the majority of my jokes.

I would like to thank Jim McAndrew and company for their XRF analyses and all of the graduate students (especially Anlin Guo, Mingzhe Zhai, and Cherylyn Skuba) for their discussion and guidance in the lab.

I would like to thank Weeks Hardware for their endless supply of cardboard boxes and rock jokes.

I would like to thank Sophie Martin for support throughout my entire university career. I would also like to extend a special thankyou to Darlene for typing and always being there when I needed you.

TABLE OF CONTENTS

LIST OF FIGURES

LIST OF TABLES

CHAPTER 1

INTRODUCTION

1.1.0 INTRODUCTION

The Grenville Province, located on the southeastern margin of the Canadian Shield, is geologically quite complex (Fig. 1.1). The Grenville encompasses approximately 1,000,000 km^2, stretching 2000 km from Labrador to south-central Ontario. Northwest of the Grenville Province lies the Archean aged Superior Province, while to the southeast, the Grenville Province is bordered by the Appalachian orogeny and overlain by Palaeozoic cover. The Grenville Province is the youngest orogeny of the Canadian Shield (Moore, 1986) and was first distinguished from adjacent regions based on structural differences and changing degrees of deformation.

The initial divisions of the Grenville are shown in Figure 1.2 (Wynne-Edwards, 1972). The author divided the Grenville into seven major sections: Grenvillian Foreland Belt, Grenville Front Tectonic Zone, Central Gneiss Belt, Central Metasedimentary Belt, Central Granulite Terrane, Baie Comeau Segment, and the Eastern Grenville Province. Of these subdivisions, only the Grenville Front Tectonic Zone

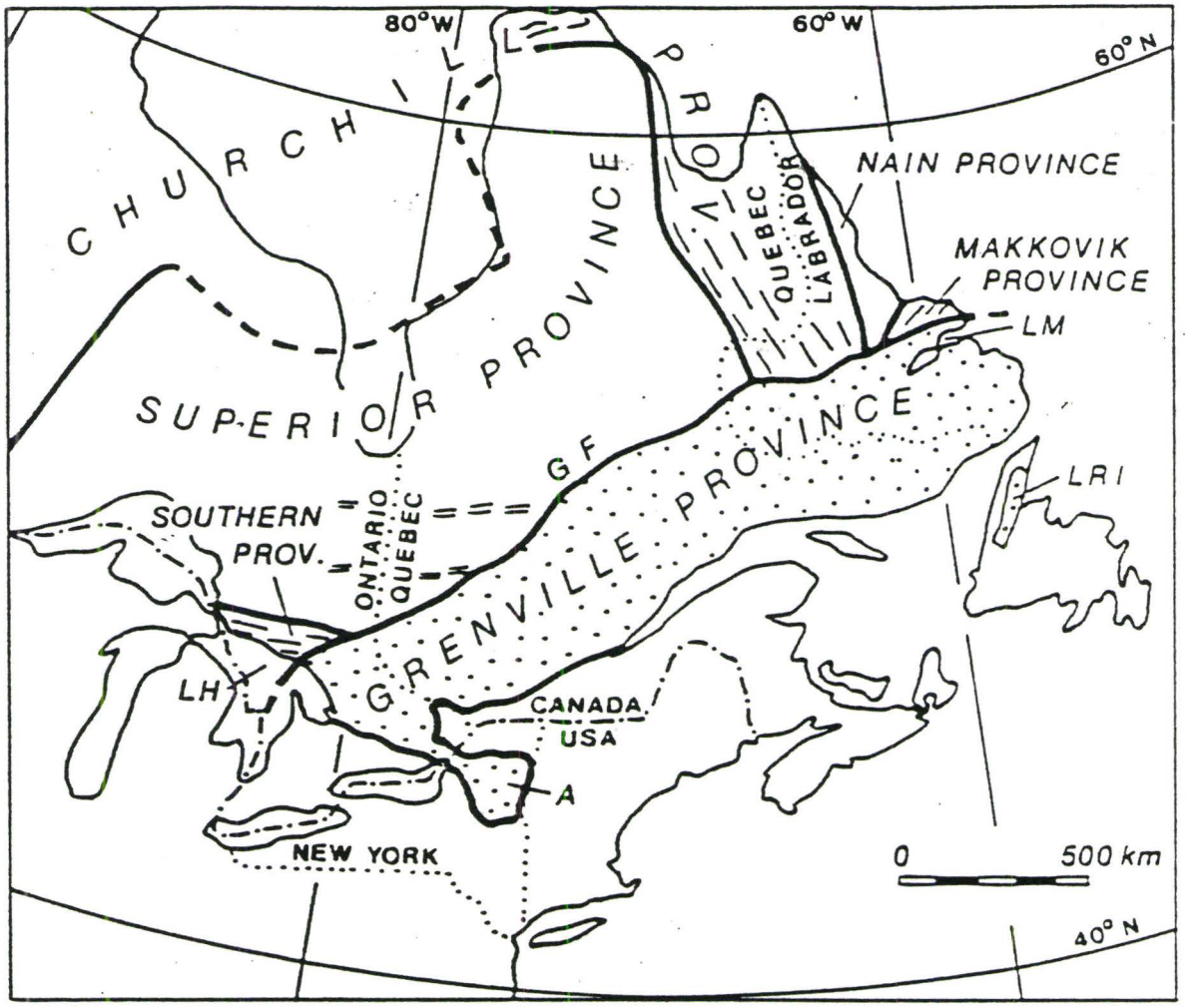

Fig. 1.1: The geographical location of the Grenville Province in Canada and the northeastern U.S. (Fig. 1 after Rivers et al., 1989).

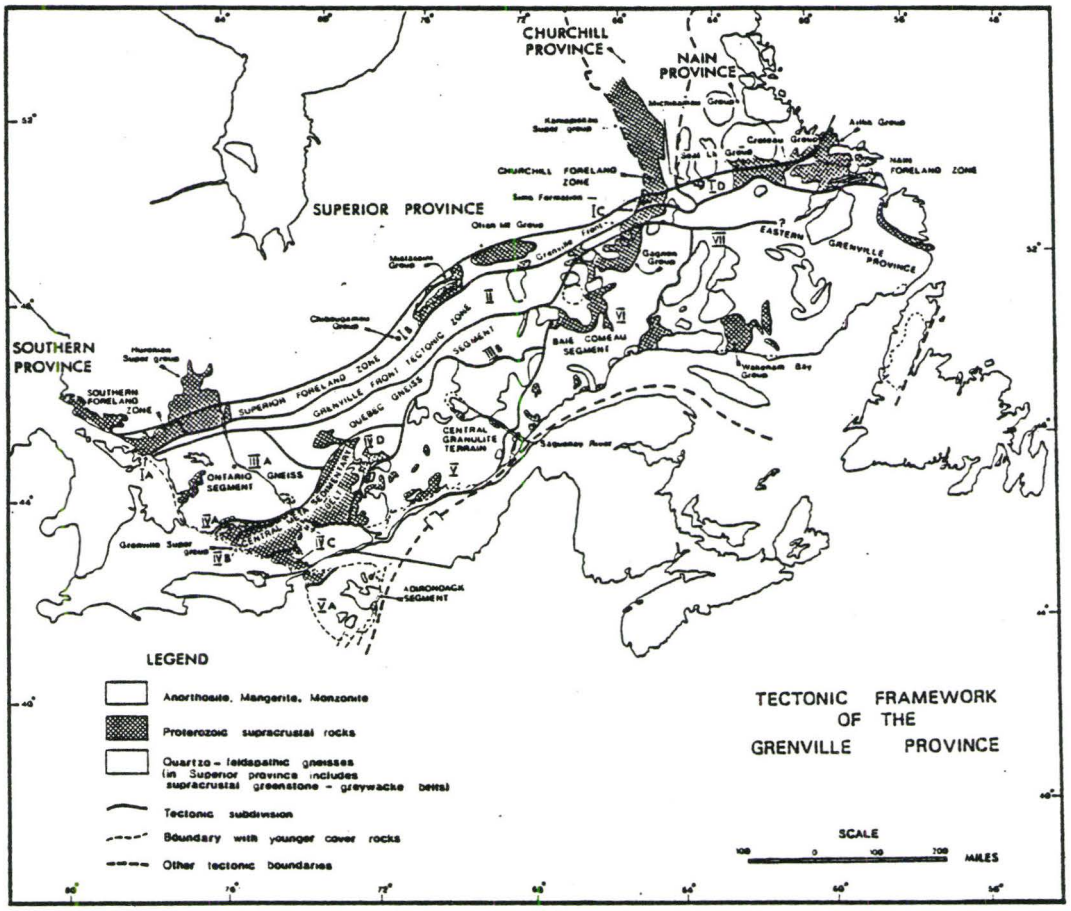

Fig. 1.2: The tectonic framework of the Grenville Province in Canada showing the initial divisions of Wynne-Edwards (1972).

(GFTZ), the Central Gneiss Belt (CGB), and the Central Metasedimentary Belt (CMB) are represented in Ontario.

A number of different workers have attempted to dissect the " geological jigsaw puzzle " in the Grenville Province using a variety of methods. For instance, Davidson (1986) and Hamner (1988) have subdivided the western part of the Central Gneiss Belt in Ontario into a series of domains and subdomains (Fig. 1.3). These lithotectonic domains and subdomains are largely a result of the Grenville orogeny which produced crustal shortening and thickening along inclined ductile shear zones. The thrusting and resultant lithotectonic domains exemplify the structural complexity of the Grenville Province.

Not only is the Grenville Province structurally complex, it is also geochronologically complex. There has been a substantial volume of geochronological work done in the Grenville Province using a variety of methods. Easton (1986) has recently documented much of the work done in the Grenville Province up until May, 1985. The data show a very wide range from K/Ar cooling ages of approximately 1.0 Ga, to igneous crystallization ages as old as 2.7 Ga. This wide range of data not only represents the different dating systems ability to withstand metamorphism, but also exemplifies the fact that the Grenville Province has suffered a polygenetic history.

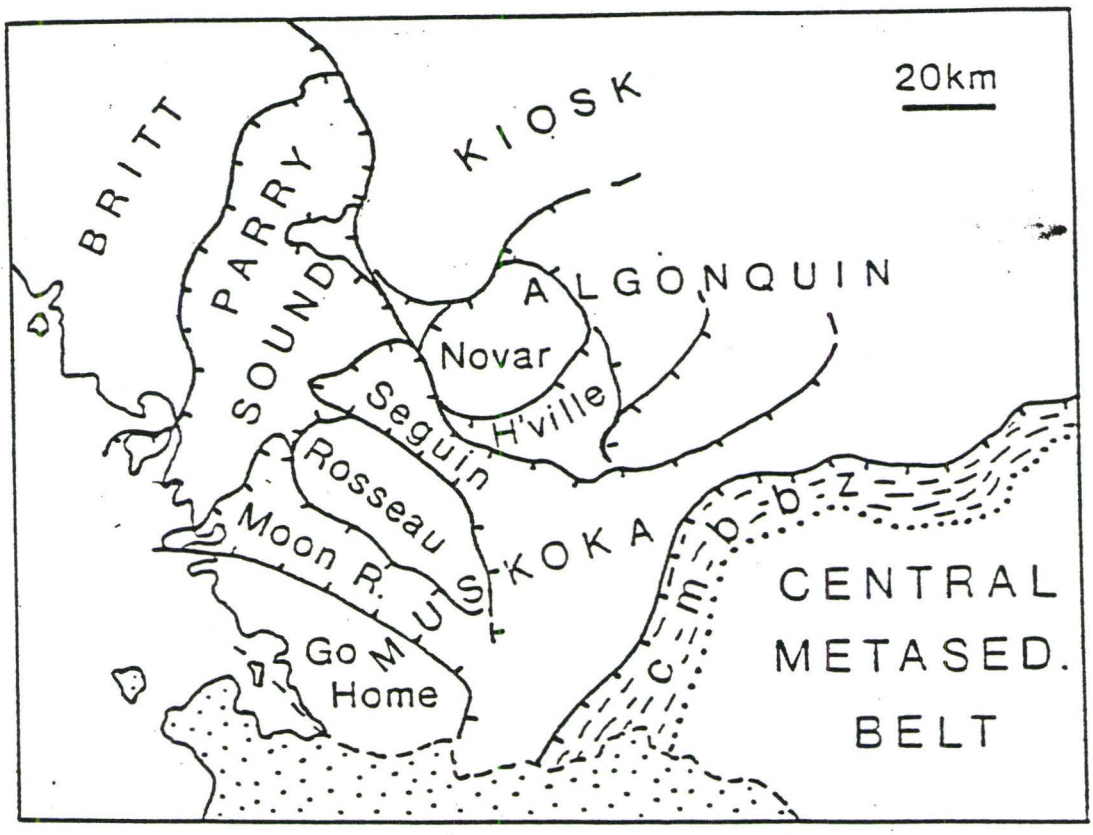

Fig. 1.3: Lithotectonic domains and subdomains of Davidson (1986) illustrating the structural complexity of the Grenville Province in the Central Gneiss Belt.

The Grenville is a multiply metamorphosed belt, representing three and maybe even four metamorphic events. While some geochronological systems register the 1.0 Ga Grenville event, other systems point towards older events. Two geochronological systems that have been used to " see through " the different metamorphic events are the Samarium-Neodymium dating system and the Lead-Lead dating system.

The Samarium-Neodymium dating system is perhaps best suited for dating high grade metamorphic rocks because Rare Earth Elements are far less mobile than other elements such as Rubidium, Strontium, and Uranium (DePaolo, 1988) during metamorphism. Samarium and Neodymium also undergo very little relative fractionation during erosional, sedimentary, and metamorphic processes (Dickin and McNutt, 1991). This realization has led a number of different workers to use Samarium-Neodymium model ages for determining the crustal extraction ages in high grade metamorphic terrains. For example, at McMaster University, Neodymium model age mapping has been used to identify a former island arc of Penokean age (1.9 Ga) in the Central Gneiss Belt (Dickin and McNutt, 1989; Holmden, 1990). The present work uses Neodymium model age mapping in the southern Central Gneiss Belt of Ontario.

1.1.1 OBJECTIVES

The objectives of the present work are three-fold:

1. To characterize the crustal formation ages of the southwestern Grenville Province in the Algonquin Park area of Ontario using the Samarium (Sm) - Neodymium (Nd) model age system.
2. To use zircon geochronology to test model age calculations.
3. To propose a tectonic model explaining the geochronological results.

In order to achieve these objectives, the work was divided into three main parts:

1. Major element analysis and subsequent petrological and tectonic discrimination diagrams.
2. Sm-Nd model age determinations.
3. Pb-Pb direct evaporation method for dating zircons.

1.1.2 THE FIELD AREA: ALGONQUIN PARK AREA, ONTARIO

The field area covers approximately 8000 km^2 and is located within the Central Gneiss Belt (CGB) of the Grenville Province, between the cities of Pembroke to the east and Huntsville to the west.

The field area is dominated by high grade para and orthogneisses, with scattered younger intrusions, pegmatites, and dikes. Much of the region has been stated to be part of the " Algonquin Batholith " (Schwerdtner and Lumbers, 1980). Although there are a considerable number of metaplutonic rocks present, there is also a fair portion of metasedimentary rocks present, implying that the Algonquin Park area is not simply one large batholith, but instead, the area represents a series of smaller plutons with sediments interspersed (Davidson and Grant, 1986).

Nd model age studies have been carried out to the north (Holmden, 1990) and to the west (Dickin and McNutt, 1991). The complex structural mapping for the majority of the field area has not been done. However, the western portion of the field area has been structurally mapped to reconnaissance standards by Davidson and Grant (1986). The lithologies of the field area are dominated by ortho, and paragneisses. The orthogneisses are largely composed of tonalite, granodiorite, and monzonite, with lesser volumes of

granites. The paragneisses are dominated by quartzofeldspathic gneisses with lesser volumes of quartzites and marbles. In a few locations, younger Sudbury diabase dikes have intruded the existing rocks. The eastern part of the field area is partially covered by drift, with few basement exposure locations. The southern portion of the field area is truncated by the Central Metasedimentary Belt Boundary Zone (CMBBZ). The CMBBZ is thought to represent a major southeast dipping, upper amphibolite facies ductile shear zone with a northwestward sense of overthrusting involving tonalitic and syenitic crystalline thrust sheets together with marbles and metapelites of the Grenville Supergroup (Hamner, 1988). Zircon dating of syntectonic pegmatites indicates that the ductile thrusting was already active in the Central Gneiss Belt at 1160 Ma (van Breeman et al., 1986). Since the rocks south of the CMBBZ likely represent younger material thrusted northwestward during the Grenville orogeny, the majority of samples were obtained north of the CMBBZ. The northern portion of the field area was contained within Algonquin Provincial Park. Few samples were obtained from this area because of the limited number of access roads.

The predominate metamorphic grades in the field area are granulite and upper amphibolite facies. There were several locations containing migmatitic rocks, indicative of partial

melting. Other locations contained charnokitic rocks indicative of granulite facies dehydration. Collecting samples from these rock types was avoided because partial melting and dehydration may fractionate Rare Earth Elements and hence, produce anomalous Nd model ages.

The extreme degree of deformation has made the area difficult to map. However, Davidson and Grant (1986) have recognized a new subdomain: the Opeongo domain, contained within the Algonquin domain as defined by Culshaw et al., (1983). The majority of the field area lies within the newly defined Opeongo domain. However, parts of the field are also located in the McLintock subdomain and the Muskoka domain (Fig. 1.4).

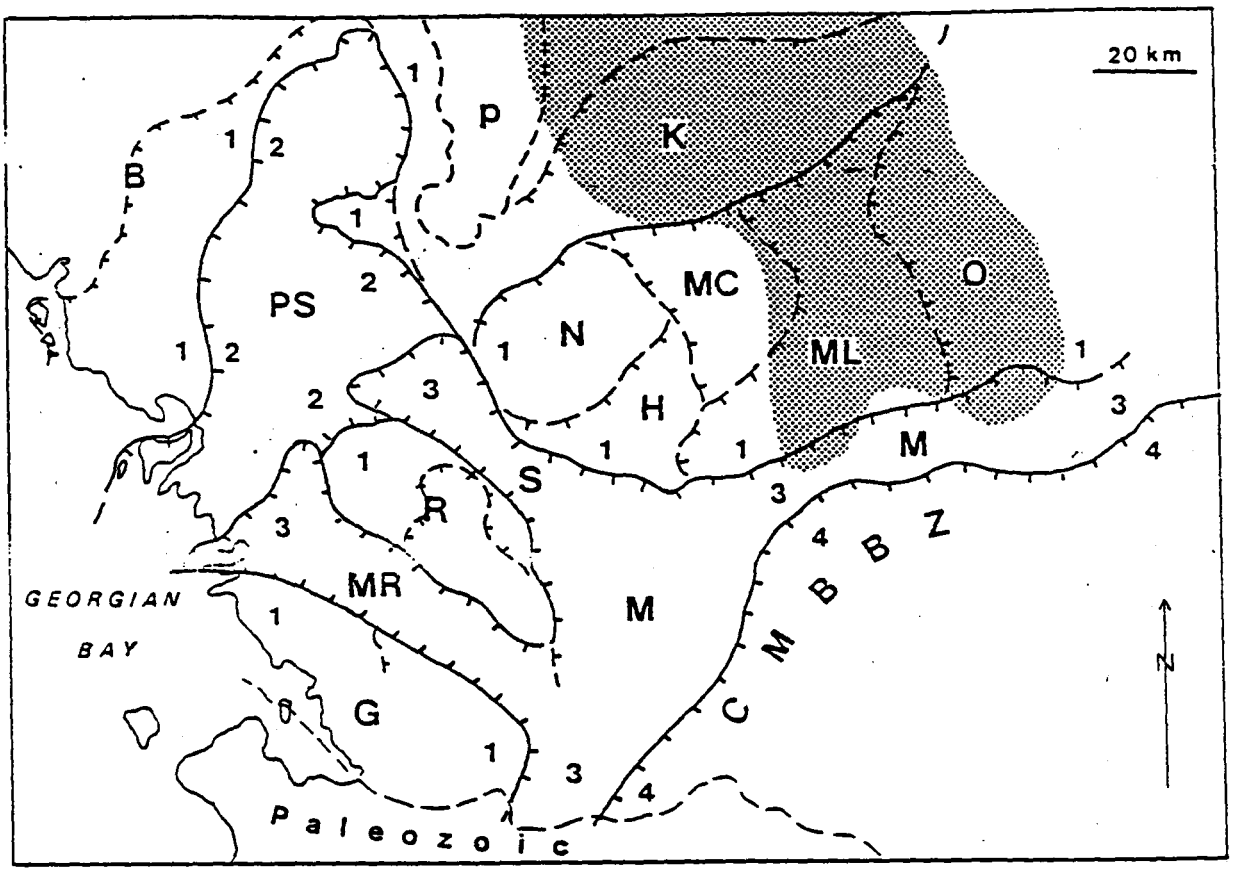

Fig. 1.4: Lithotectonic domains and subdomains of Davidson and Grant (1986) showing the newly defined Opeongo subdomain of the Algonquin domain. Stacking order due to Grenville thrusting is also shown. Stack 1: B - Britt, K - Kiosk, R - Rosseau, G - Go Home, N - Novar, H - Huntsville, Mc - McCraney, ML - McLintock, O - Opeongo. Stack 2: PS - Parry Sound. Stack 3: M - Muskoka, Mr - Moon River, S - Seguin. Stack 4: CMBBZ - Cental Metasedimentary Belt Boundary Zone. Shaded area indicates field area of Davidson and Grant.

CHAPTER 2

2.1.0 TECTONIC SETTING: THE GRENVILLE PROVINCE

The Grenville Province is the youngest orogenic belt of the Canadian Shield. The Grenville orogeny has been dated at 950 +/-150 Ma using K/Ar cooling ages (Stockwell, 1964). The Grenville orogeny has been compared to the Himalayan continent-continent collision for two reasons. Firstly, the Grenville lacks Andean style plutonism of Grenvillian age. Secondly, a continent-continent collision can best explain the ductile thrust sheets representing the northwestward directed compression that occurred during the Grenville orogeny.

Several systems have been used to elucidate pre-Grenvillian orogenic terranes. Uranium-lead and lead-lead dating of zircons are two methods used to determine the crystallization ages of pre-Grenville orogenic rocks. Another method used is the Nd model age system. The Nd model age system has been applied to country rock gneisses to determine crustal residence ages of pre-Grenvillian terranes (Dickin and McNutt, 1989; Dickin and McNutt, 1991; Dickin and Higgins, 1992). The Nd model age system has also been used elsewhere. For instance, in the mid North American continent by DePaolo (1981c) and Nelson and DePaolo (1985).

Recent discovery of lithotectonic domains by Davidson

(1986) and Hamner (1987) has drastically changed the original map of the Grenville (Wynne-Edwards, 1972). Rivers et al., (1989) have developed a new tectonic framework for the Grenville. The new divisions differ from those of Wynne-Edwards (1972) and are based on geological, geophysical, and geochronological data. The new divisions define three first order tectonic boundaries separating three first order longitudinal belts (Fig. 2.1):

Grenville Front: marks the northwesterly limit of Grenville metamorphic and deformational effects.

Parautochthonous Belt: up to 150 km wide and lies between the Grenville Front and the Allochthon Boundary Thrust. It contains a number of Archean and Proterozoic terranes that are separated by second order boundaries.

Allochthon Boundary Thrust: divides the Parautochthonous Belt to the north, from the allochthonous terranes to the south. It is thought to represent a locus of major thrust displacements to the northwest. The Allochthon Boundary Thrust also corresponds to a break in isotopic ages.

Allochthonous Polycyclic Belt: is a belt of transported terranes tectonically overlying the Parautochthonous Belt.

The terranes represent pre-Grenvillian accretions and

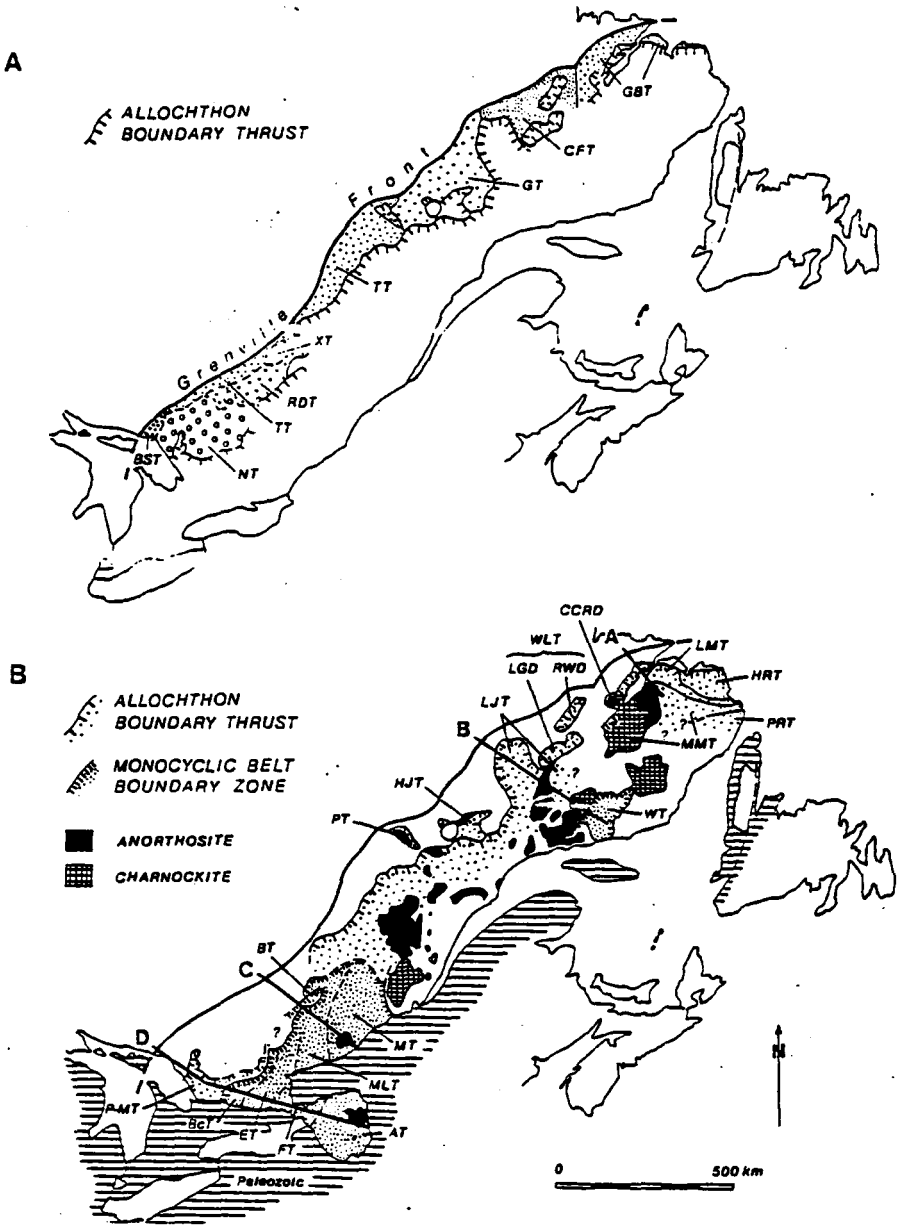

Fig. 2.1: The new tectonic divisions of the Grenville Province (after Rivers et al., 1989).

orogenies.

Monocyclic Belt Boundary Zone: separates the polycyclic rocks to the north and the monocyclic rocks (i.e.- only showing Grenvillian related tectonics) to the south.

Allochthonous Monocyclic Belt: is a series of terranes containing only Grenvillian related tectonic signatures. Represented in the southwestern Grenville as the Central Metasedimentary Belt.

2.1.1 THE CENTRAL GNEISS BELT

The Central Gneiss Belt in Ontario extends across the province, from Georgian Bay to Quebec. To the north lie the Huronian metasediments of the Superior Province, while to the south lie the Grenville Supergroup of the Central Metasedimentary Belt. The Central Gneiss Belt represents a series of mid-crustal, northwest thrusted slices displaced during the Grenville orogeny. However, the wide range of ages present in the Central Gneiss Belt suggests that the genesis of the area is far more complex than mere Grenville thrusting. From chronological techniques such as zircon dating and Nd model age dating, it has been proposed that the Central Gneiss Belt represents a series of older orogenies and island arcs that collided with the North American craton margin during the Proterozoic. This work has attempted to chronologically

analyse the southern portion of the Central Gneiss Belt in the Algonquin Park area of Ontario.

CHAPTER 3

THE Nd MODEL AGE CONCEPT

3.1.0 Nd MODEL AGES

The ages obtained from Nd model age dating represent the time at which the rocks in question separated from a homogeneous depleted mantle reservoir and became incorporated into the Earths crust. The Earths crust has evolved through time by selective removal of lighter elements from the mantle. The " melting off " of the lighter elements from the Earths mantle has produced lighter, more buoyant fractions. These buoyant fractions have resisted subduction through time because they are less dense than the remaining mafic material present in the mantle. In turn, the lighter fractions have amalgamated together to form continents. The continents are essentially the only record of the past geological events that have occurred on the Earths surface.

The remaining mantle material thus loses portions of the lighter continental material. Although some light continental material may get subducted at convergent plate boundaries, most lighter material remains on the Earths surface. The net result is the generation of a mantle depleted in lighter elements.

Not only is the mantle depleted of lighter elements, it

is also depleted in large ion lithophiles. Included in these large ion lithophiles are some of the incompatible elements that are the first elements " melted off " and the last elements to solidify during the evolution of a magma body. For example, Rare Earth Elements such as Sm and Nd reflect these fractionation affects that are known to occur in the Earths mantle.

There are a number of different models thought to represent the changing composition of the Earth's interior through time. When the Earth formed 4.6 Ga ago, it is believed that Sm and Nd condensed early from the cooling solar nebula (Grossman and Larimer, 1974). Hence, fractionation of Sm and Nd during condensation of the solar nebula should have been negligible because both elements were quantitatively transferred into the early formed solid bodies that later accreted to form planets (DePaolo, 1988). Thus, most of the variations of Sm/Nd ratios in the earth today are a result of the Earths internal differentiation.

Earlier models for the evolution of the Earths interior were based on isotopic ratios of chondritic meteorites. Chondritic meteorites are thought to represent the "original" nebular compositions because they not only contain refractory elements, but also contain volatiles, suggesting that the chondrites have not undergone substantial fractionation. These observations have given rise to the CHUR (CHondritic

Uniform Reservoir) model for the isotopic evolution of Sm and Nd. Sm/Nd radiogenic ages determined for a rock based on the CHUR model utilize the undifferentiated Sm/Nd ratios found in chondrites. However, unlike the chondrites, the Earth has differentiated through time. Thus, the Sm/Nd evolution in the fractionated mantle differs from the Sm/Nd evolution in unfractionated chondritic meteorites. This has given rise to the Time Dependent Depleted Mantle Model (Tdm) (DePaolo, 1981a) (Fig. 3.1). For rocks younger than 2.7 Ga, the Depleted Mantle Model is preferred, while for rocks older than 2.7 Ga, the CHUR model is used.

The curvi-linear trend for the mantle evolution line was determined by measuring Nd ratios in island arc rocks 1.8 Ga old, and present day island arc rocks. A third point corresponded to Nd ratios 4.6 Ga ago. A curve was then fitted to these three points, representing the evolution of Nd ratios of the mantle through time. Island arcs were used because they are thought to directly sample the magma forming mantle itself.

The Sm-Nd model age system is based upon the radiometric decay of ^{147}Sm to ^{143}Nd. Although the half-life of this decay is 106 Ga, it is still short enough to produce measurable differences in parent-daughter isotope ratios. There are also several none-radiogenic Nd isotopes such as ^{144}Nd. Thus, by measuring the present day $^{143}Nd/^{144}Nd$ ratio

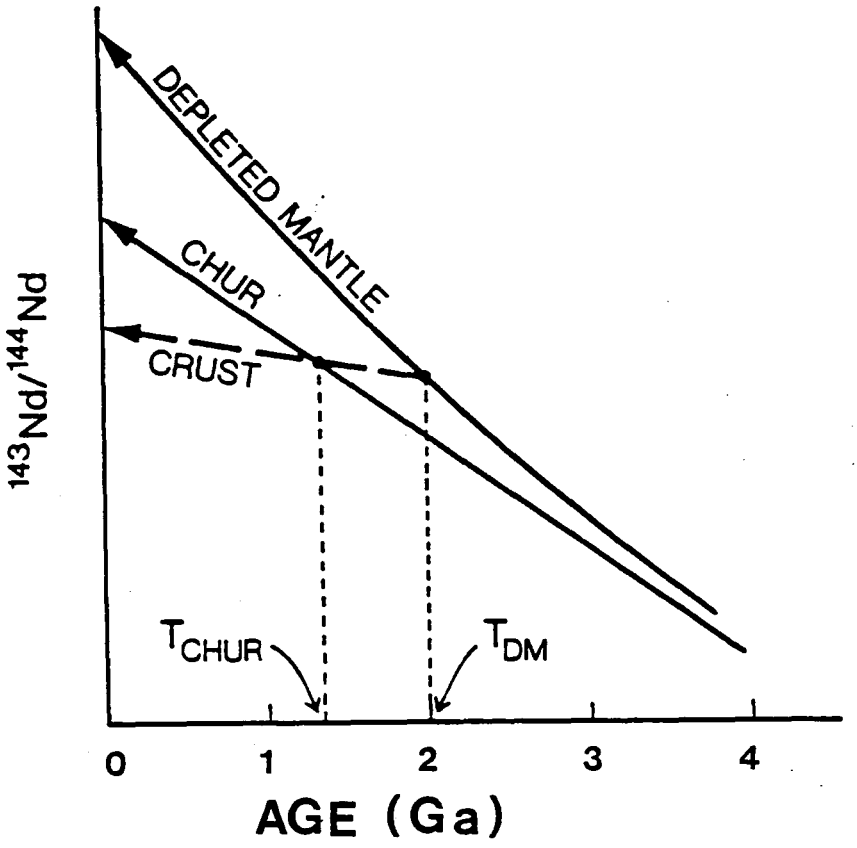

Fig. 3.1: Illustration showing the isotopic evolution of Nd for the CHUR model as well as the Depleted Mantle model. The diagram shows the large difference in model ages calculated using the Depleted Mantle model and the CHUR model for a hypothetical sample (after DePaolo, 1981c).

along with the Sm and Nd concentrations of the rock in question, it is possible to extrapolate the Nd evolution line back to its intersection with the Depleted Mantle curve. The intersection defines the crustal formation time for the crust forming magma. The differences between T_{DM} and T_{CHUR} are best exemplified in a plot of Epsilon-Nd vs. time (Fig. 3.2). Epsilon-Nd is essentially a magnified difference between the $^{143}Nd/^{144}Nd$ ratio of the sample and CHUR at some time in the past.

Sm and Nd experience very little relative fractionation during intra-crustal events such as erosion, sedimentation, and metamorphism. However, Sm and Nd undergo substantial fractionation during crustal extraction from the mantle. Therefore, magma separated from a homogeneous mantle reservoir will become preferentially enriched in Nd over Sm. The magma will thus define a new Nd evolutionary trend. Where the new Nd evolutionary trend intersects with the Depleted Mantle curve, the initial $^{143}Nd/^{144}Nd$ ratio is defined and hence, the age of the new crustal package.

However, there are several assumptions inherent to the Nd model age approach (Arndt, 1987):

1. Isotopic evolution of the mantle source is known.
2. The time of mantle extraction and crustal emplacement and crystallization is short.
3. The Sm/Nd ratio of the rock forming magma has not

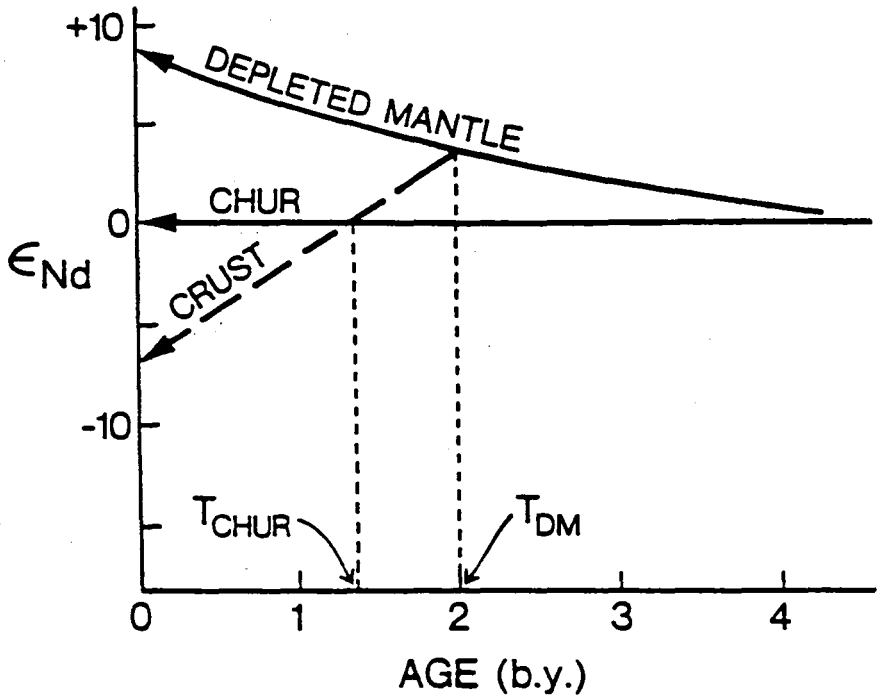

Fig. 3.2: A plot of Epsilon-Nd vs. time depicting the changing Epsilon-Nd values through time.

$$\text{Epsilon-Nd (T)} = 10^4 \left(\frac{^{143}Nd/^{144}Nd_{sample} - ^{143}Nd/^{144}Nd_{CHUR(T)}}{^{143}Nd/^{144}Nd_{CHUR(T)}} \right)$$

been modified by later intracrustal events.

Arndt's third assumtion is perhaps the most common reason for the misinterpretation of Nd model ages. There are several intracrustal events that could alter the Nd isotope ratios. For instance, anatexis and assimilation of older or younger crust; sediment subduction at convergent plate boundaries in an orogenic setting; and paragneisses with mixed provenance sediments composed of older and younger components, are several possibilities that may produce mixed model ages (Fig. 3.3). Thus, when interpreting Nd model ages, these possibilities must be considered.

3.2.0 Nd MODEL AGE MAPPING IN THE GRENVILLE PROVINCE

There are several reasons that make Nd model age mapping a good reconnaissance tool when searching for pre-Grenvillian accretionary terranes in the Central Gneiss Belt in Ontario. For example, the high grade of metamorphism does not produce substantial fractionation of Sm and Nd. Sm and Nd are virtually immobile on a " whole rock " scale even in granulite grade rocks. Large areas may be chronologically characterized in short periods of time because fewer samples are needed to date an area as compared to the isochron method. For these reasons, several workers have used the Sm-Nd model age method in the Central Gneiss Belt. For instance, Dickin and McNutt (1991) have used Nd model ages to characterize the

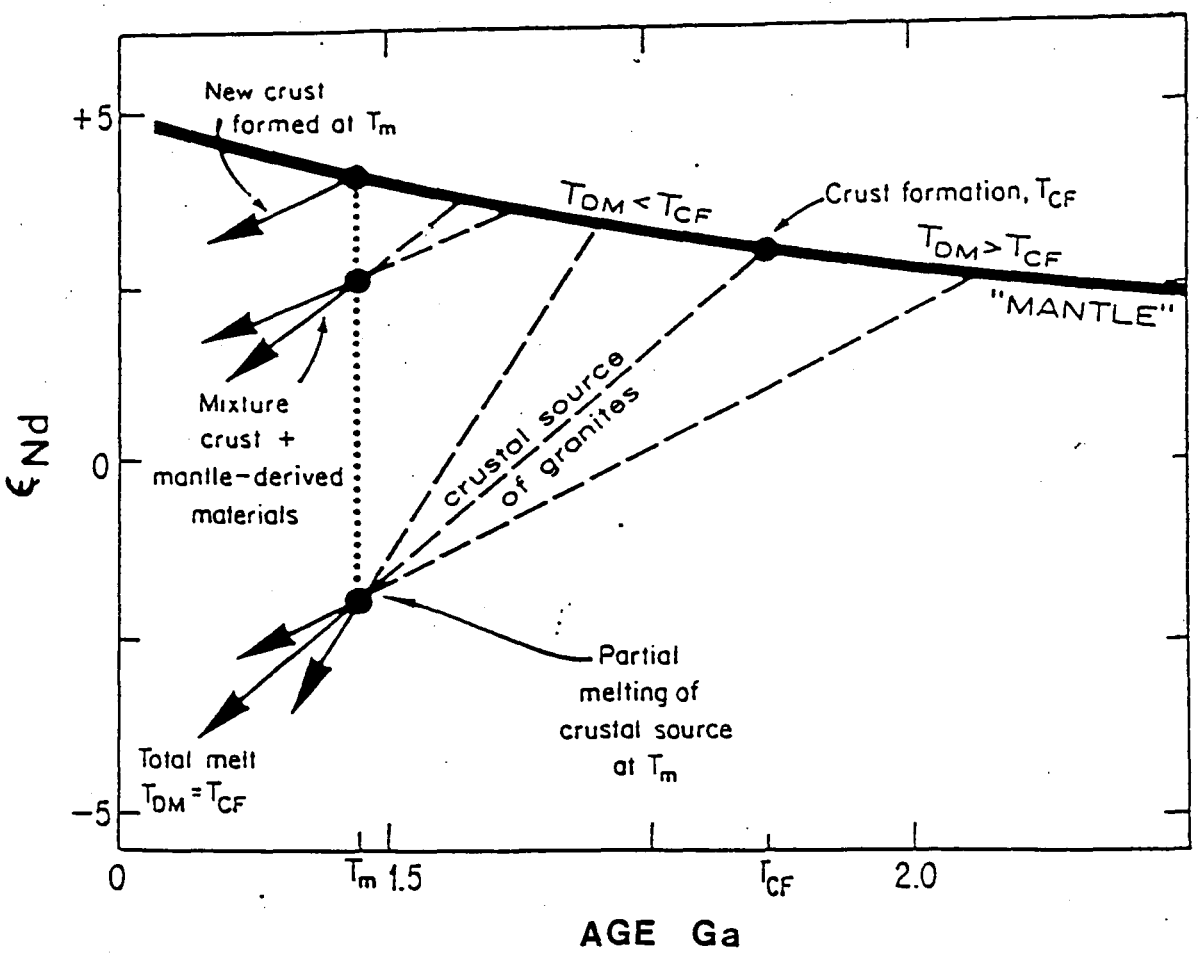

Fig 3.3: Diagram illustrating possible reasons for anomalous model ages produced from partial melting: A magma body separates from the mantle at T_{CF} and follows the " crustal source of granites " line. Then, partial melting occurs at T_M and a new Nd evolution line is produced. The same type of Nd evolution line would occur if older and younger sediments mixed together. (after Nelson and DePaolo, 1985)

lithotectonic domains of Davidson (1986) (Fig. 3.4). Nd model age mapping has also revealed a significant step in model ages in the Lake Nipissing area (Fig. 3.5) interpreted as a collisional suture between the Archean craton and an early Proterozoic island arc. A Nd isotopic study has also been done on the major plutons of the area (Dickin et al., 1990). The present study is aimed at a chronological characterization the rocks in the southern sections of the Central Gneiss Belt in the Algonquin Park area in Ontario.

There are two lines of evidence to justify the use of DePaolos depleted mantle model for the rocks in the Algonquin Park area. Firstly, in adjacent regions, model ages and isochron ages for Sm and Nd are in excellent agreement (Dickin and Higgins, 1992). Secondly, the model ages calculated were also confirmed by Pb-Pb dating of zircons. The agreement between model age, isochron age, and zircon age, is justification for the correctness of DePaolos derivation of the depleted mantle as a model of the crust forming reservoir of the Central Gneiss Belt in the southwestern Grenville Province.

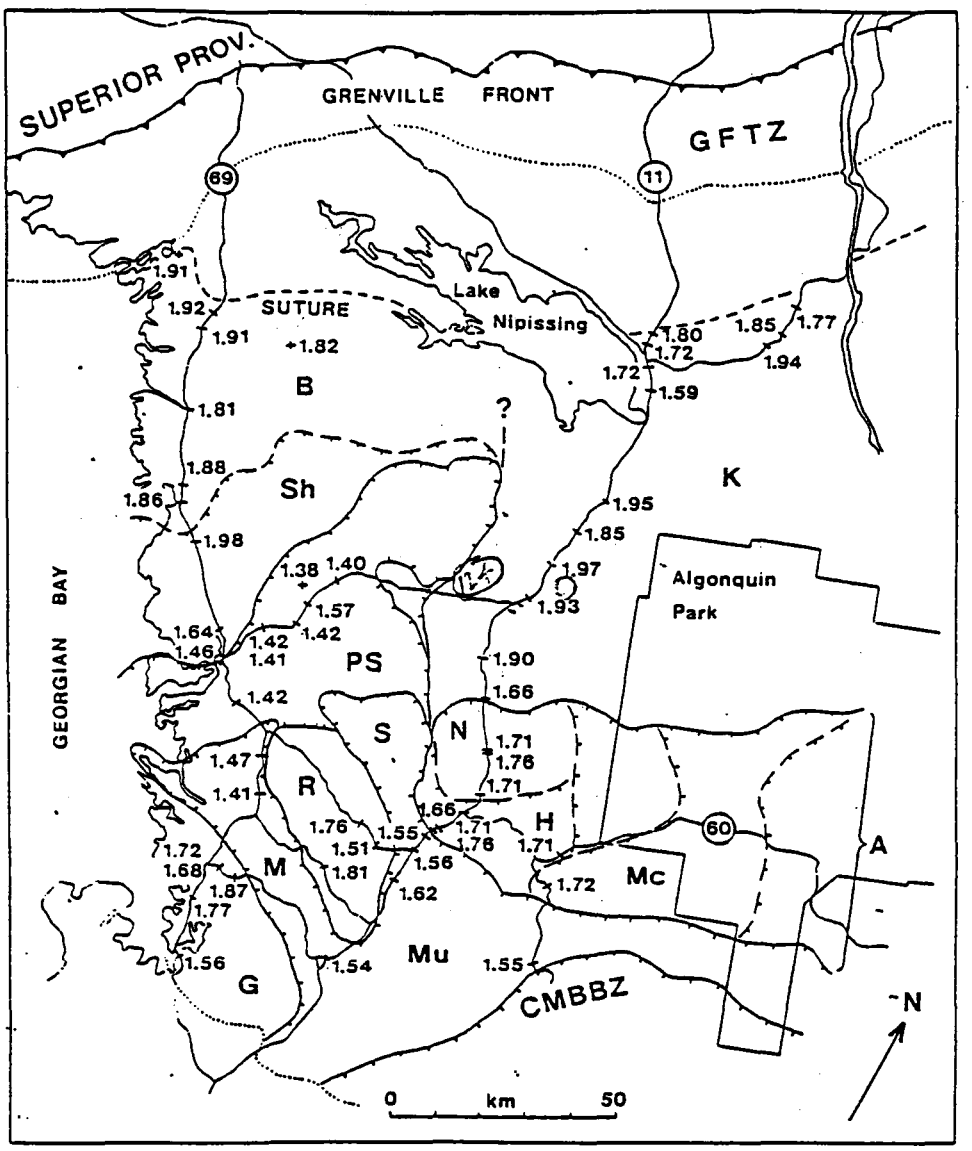

Fig 3.4: Nd model age characterization of the lithotectonic domains of Davidson (after Dickin and McNutt, 1991).

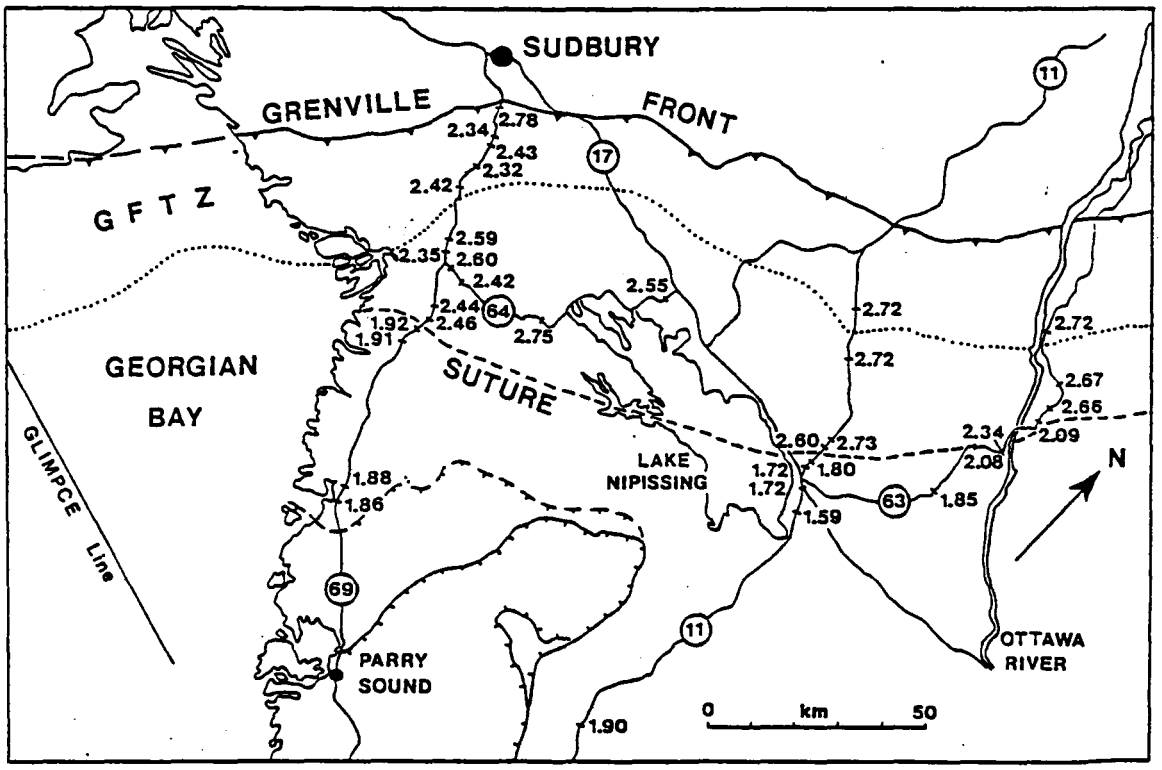

Fig. 3.5: Map illustrating the collisional suture between an early proterozoic island arc with the Archean foreland (after Dickin and McNutt, 1989).

CHAPTER 4

Pb-Pb ZIRCON DATING BY DIRECT EVAPORATION

The Pb-Pb dating method is based on the decay of ^{238}U and ^{235}U to ^{206}Pb and ^{207}Pb respectively. Since the rate of decay of U to their respective Pb daughter products is known, it is possible to determine the age of the rock or mineral in question. Zircons are ideal minerals for Pb-Pb dating because zircons do not readily incorporate Pb into their lattices during crystallization. The only Pb that is usually present in a zircon is Pb that has been incorporated in inclusions and Pb produced by the radioactive decay of U. In order to accurately date the zircons, the Pb incorporated in the inclusions, which can be identified by high concentrations of ^{204}Pb, must be subtracted. The concentration of common Pb in the zircons was estimated using Stacey and Kramers (1975) approximation of terrestrial Pb. The common Pb points were used to determine the slopes and intercept ratios for each zircon on a $^{207}Pb/^{206}Pb$ vs. $^{204}Pb/^{206}Pb$ plot.

The mass spectrometer measured six different Pb masses: 203.5, 204, 204.5, 206, 207, and 208. The 203.5 and 204.5 measurements were used to detect the level of background. The computer program then calculated the ratios and error for $^{207}Pb/^{206}Pb$, $^{204}Pb/^{207}Pb$, $^{204}Pb/^{206}Pb$, and $^{204}Pb/^{208}Pb$. The mass

calculations were done ten times (= 1 block) and the mean and standard error (%) were determined for each zircon. Each block was considered as a single point on the $^{207}Pb/^{206}Pb$ vs. $^{204}Pb/^{206}Pb$ graph. The number of blocks differed from zircon to zircon.

For each zircon, the common Pb point was determined. Isochrons with two or more points were estimated by a York fit (York, 1969) of the data. The $^{207}Pb/^{206}Pb$ intercept ratio was used to determine the age of each zircon. A complete account of the error analysis can be found in Mueller (1991).

The Pb-Pb direct evaporation method was used because of the ease of zircon analysis. Unlike the U-Pb method for zircon dating, the Pb-Pb method requires very little chemical preparation of the zircons. Although the Pb-Pb method does not allow the determination of which zircons are concordant vs. discordant, the Pb-Pb method does allow rapid analysis in minimal time. Any zircons that may be discordant were recognized by a spread in their ages, and attributed to Pb loss through time. Thus, the oldest zircon ages were regarded as the crystallization age for the rock in question. Due to the high grades of metamorphism for the samples, any younger ages were the result of either Pb loss or metamorphic overgrowths and grains formed during younger events.

There was one main reason for dating the zircons. The zircon ages determined can be used to reinforce the model ages

as representing a real geological event. For example, if the zircon age and the model age for the same sample are within error, then this implies that the Depleted Mantle model of DePaolo is a true representation of the rock forming reservoir.

CHAPTER 5

ANALYTICAL PROCEDURES: Sm-Nd

5.1.0 INTRODUCTION

The analytical procedures for Sm-Nd geochronology may be divided into three main parts: field sampling and rock crushing, dissolution and cation chromatography, and mass spectrometry. The analytical procedures will be described in chronological order.

5.1.1 SAMPLING AND ROCK CRUSHING

The gneissic samples obtained in the field varied from 5 to 10 kg in mass and were collected at roadside outcrops. At all sites, the samples collected were as representative of the outcrop as would allow and were as homogeneous as possible. The weathered material was removed and care was taken not to contaminate the sample with the local soil or organic material.

In the rock crushing laboratory, the samples were first broken down to 1 to 2 kg pieces with a 2 pound sledge hammer. The samples were then broken into smaller hand sample sized pieces with a hydraulic splitter. From the hydraulic splitter, the samples were pulverized with a jaw crusher into gravel that measured less than 1 cm on a side. The jaw crusher was first pre-contaminated with some of the sample in

order to avoid any contamination from previous samples. The gravel obtained from the jaw crusher was then split several times with a table top divider. After splitting, the remaining 100 to 200 ml of gravel was loaded into a tungsten carbide disc mill which was then placed in a shatterbox. The shatterbox was operated for approximately 5 minutes, producing a fine sand. The entire sample was then removed from the disc mill and poured onto a clean sheet of paper. About one half of the powder was then re-loaded into the disc mill while the remaining half was discarded. The shatterbox was operated for another 6 to 8 minutes until a fine powder of approximately 300 mesh was produced. The resulting 80 to 100 ml of fine powder was then poured into a 125 ml glass container, ready for dissolution.

Between each sample preparation, all equipment and working surfaces were carefully cleaned first with a vacuum and then wiped clean with disposable paper towels.

The jaw crusher was dismantled and the crushing plates were scrubbed with a wire brush. The plates were then vacuumed, along with the rest of the jaw crusher, and finally wiped clean of all grit. Similarly, the disc mill was thoroughly vacuumed and wiped free of any dust before the next sample was loaded. Polyethylene gloves were worn, ensuring that no dust-attracting skin oils were deposited on the tungsten carbide ring and puck. The table top divider was

vacuumed and an air hose was used to clean the divider chutes. At all times, the volume of airborne particles was kept at an absolute minimum so as to ensure each sample was free from contamination.

5.1.2 DISSOLUTION AND CATION CHROMATOGRAPHY

Before dissolution of the samples, the samples were accurately weighed with a balance. Prior to weighing, the balance was levelled and static was removed. The teflon bombs used for dissolution were also freed of static electricity. This allowed fast, accurate measurements to be made. The empty teflon bomb was weighed twice to ensure all static had been removed. If the weight was discrepant to more than 0.0002g, then more static was removed from the bombs. Once the bombs were free from static, between 70 and 150 mg of powder was weighed in each bomb and approximately 10 ml of concentrated HF (48%) was added. The teflon bombs were then tightly sealed and placed into teflon safety jackets. The safety jackets and bombs were placed in an oven and left for 3 days at 140°C.

After 3 days, the bombs were removed, cooled, and the Hf was evaporated on hot plates enclosed in a laminar flow hood. When the samples were dry, about 5 ml of concentrated HNO_3 (16 M) was added to each bomb and then evaporated. 5 ml of 6 M HCL was added and the bombs were put back into the safety jackets and replaced in the oven overnight. Next day, the

samples were cooled and diluted with approximately 5 ml of milli-Q water. If there were no undissolved residues remaining, then the samples were ready to be split and spiked.

Each bomb was weighed and the mass recorded. Approximately one half of each diluted sample was poured into separate 15 ml teflon beakers and the bombs were re-weighed. Approximately 5 drops of a mixed REE spike, enriched in Sm and Nd, was added to each of the 15 ml beakers. Solutions in both the bombs and the beakers were then evaporated to dryness and redissolved with 2 ml of 2.5 M HCL. The aliquots were then transferred to plastic test tubes and centrifuged for 10 minutes. The samples were now ready for cation chromatography.

There were 2 steps in column chromatography. The first step involved separation of major elements such as Na, K, and Ca, from the REE (Cation exchange chromatography) while the second step involved separation and concentration of Sm and Nd (REE chromatography).

CATION EXCHANGE CHROMATOGRAPHY: 1 ml of sample was loaded onto columns (30 cm x 0.5 cm I.D.) containing approximately 18 cm of Dowex Bio-Rad AG 50W (200 - 400 mesh) resin. The major elements were removed from the sample by eluting 2.5 M HCL and then 2 M HNO_3 on a polystyrene sulphonic acid resin. The REE remaining in the column were then collected with 7.5 M HNO_3. The REE solutions, after being evaporated to dryness, were

redissolved in 1 ml of 0.2 M HCL and then loaded onto the REE columns.

REE CHROMATOGRAPHY: Three different solutions were collected from the REE columns. The REE were separated in quartz columns in a hexyl di-ethyl hydrogen phosphate medium, coated onto teflon beads. Nd used for isotope dilution analysis was collected with 0.2 M HCL. Sm used for isotope dilution analysis was collected with 0.5 M HCL. Since the LREE are collected before the HREE, this is referred to as " the reverse phase method ". Other methods usually collect Sm first.

These three solutions were then evaporated down and 2 drops of 3 M HNO_3 with 1.3% H_3PO_4 was added and partially evaporated again. This helps to redissolve the crystalline residues in 0.3 M H_3PO_4 when the samples are loaded onto filaments for mass spectrometry.

5.1.3 MASS SPECTROMETRY

Before the samples were loaded onto the Tantalum side filaments of a Rhenium-center, Tantalum-side, glass bead, the beads and filaments were outgassed under a vacuum. A complete account of bead preparation is given in Thirlwall (1982). Then, approximately 1/2 microlitre of 0.3 M H_3PO_4 was used to dissolve the samples. This acid-sample solution was loaded onto the Tantalum side filament and dried by applying 2.0-2.5 amps to the Tantalum filament.

All Nd-Sm isotope ratios were performed on a VG 354 solid source mass spectrometer. All analyses were done at source pressures < 2.0×10^{-7} bars. Isotope dilution analyses of Sm and Nd were measured using a mixed ^{149}Sm-^{150}Nd spike. Nd isotope ratios were normalized against a $^{146}Nd/^{144}Nd$ ratio of 0.7219. 25 runs of the La Jolla standard produced a $^{143}Nd/^{144}Nd$ mean of 0.511854 +/- 0.00004 (2σ). No isotope dilution data was accepted with within run standard errors of > 0.02 %. No Nd isotope ratio data was accepted with within run standard errors of > 0.01 %. Thus, the resultant uncertainty for the model ages calculated was approximately +/- 20 Ma (2σ).

CHAPTER 6

ANALYTICAL PROCEDURES: ZIRCON DATING

6.1.0 INTRODUCTION

The analytical procedures for Pb-Pb zircon dating by direct evaporation may be divided into three main parts: zircon separation, zircon loading, and mass spectrometry. The analytical procedures will be described in chronological order.

6.1.1 ZIRCON SEPARATION

Selected samples were powdered using a ceramic disc mill in order to obtain a grain size between 24 and 100 mesh. Between samples, the disc mill was vacuumed clean and blown free of dust using an air hose. The fine sand obtained from the disc mill was then processed using a shaker table. The shaker table removed the majority of the lighter grains such as feldspar and quartz. The heavier grains of magnetite, biotite, zircon, and amphibole were collected from the shaker table by adjusting the shaking and water flow of the table. The heavy fraction grains were then dried down and a hand magnet was used to remove the highly magnetic grains such as magnetite and biotite. Further separation of lighter material was achieved by using the heavy liquid sodium polytungstate.

The density of this heavy liquid (3.0 g/cm^3) was sufficiently high enough so as to remove a large portion of the remaining quartz grains. The heavy mineral fraction was collected from the sodium polytungstate and thoroughly rinsed with distilled water. After drying the remaining sample, a Franz magnetic separator was used to separate any existing weakly magnetic material. The non-magnetic fraction was collected and transferred to a microscope. The zircons in the remaining portion were removed by hand picking. The largest and most inclusion free zircons were chosen because these zircons will have suffered minimal Pb loss.

6.1.2 ZIRCON LOADING

The zircons were loaded onto the side filament of a zone refined, wide (0.05") Rhenium filament welded onto standard triple filament glass beads. Each zircon was wrapped securely in the side filament by firstly making a trough-like shape in the filament, and secondly, crimping the top of the filament with the zircon grain inside the trough. A second wide Rhenium filament was added vertically at the centre posts of the glass bead. This filament would serve as a deposit site for Pb evaporated from the side filament (Fig. 6.1). The posts were then bent so that the centre and side filaments were as close to one another as possible (0.5-1.0 mm).

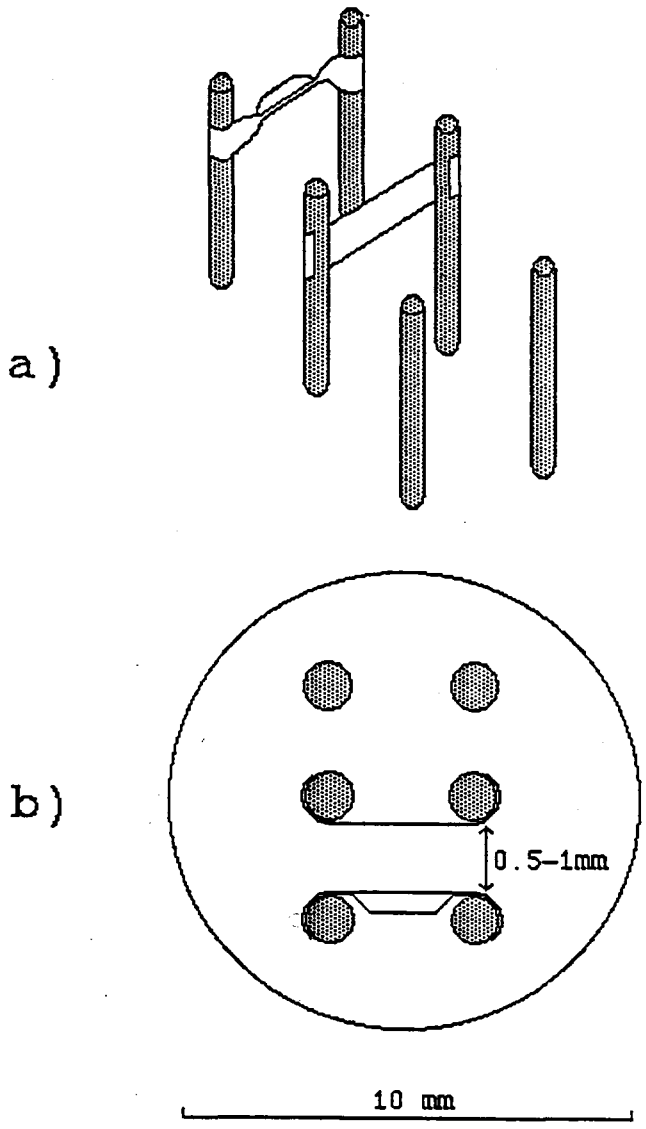

Fig. 6.1: Diagram of the beads used for zircon dating (after Mueller, 1990).

6.1.3 MASS SPECTROMETRY

The zircons were analyzed at McMaster University on a VG 354 solid source mass spectrometer. The analysis for each zircon was as follows:

1. Centre and side filaments were cleaned by passing a 5.0 amp (centre) and 3.0 amp (side) current through them.
2. The side filament was heated until a beam had been achieved (10-15 minutes).
3. The beam was allowed to deposit Pb onto the centre filament for a few runs with the side filament off.
4. The centre filament was then heated and the Pb deposited from the side filament, was emitted in a steadier stream as compared to the side filament beam.
5. These evaporation and deposition steps were continued until no more Pb beams were produced.

If the beam from the side filament was stable enough, then it was used for data collection. However, usually the centre filament beam was better, producing more precise data.

When the zircon was finished, the filaments were cleaned by passing a high current through them so that the beads could

be used again. Throughout the procedure, the current was controlled manually. To avoid collecting Pb data from metamorphic rims that may have been present on the zircons, the computer program was paused for a brief moment so as to allow enough time to drive off the metamorphic Pb. Only the zircon data with low concentrations of ^{204}Pb was used in the age determinations.

CHAPTER 7

RESULTS

7.1.0 Nd MODEL AGE MAPPING

In the Algonquin Park area of Ontario, a total of sixty new samples were collected. Of the sixty samples, forty-nine Nd model ages were determined. Forty-two of the forty-nine model ages calculated were north of the CMBBZ. These forty-two samples were added to thirteen samples previously determined by Dickin and McNutt (1991) and fifteen unpublished samples. The samples located south of the CMBBZ are not plotted on the compilation map (Fig. 7.1) but are included in the table of isotopic data for completeness (Table 7.1).

From the compilation map, it is readily seen that the Algonquin area is composed of mixed model ages. There is no obvious step-wise decrease in model ages that may represent a collisional suture between the early Proterozoic foreland and a mid Proterozoic island arc. Instead, the model ages have a wide temporal distribution over a small area. This is best exemplified in the histogram of all data obtained (Fig. 7.2). Because the rocks in the field area have been subjected to amphibolite and granulite metamorphic grades, distinguishing between metaplutons and metasediments is

Fig. 7.1: Compilation map of the field area showing the model ages and their locations.

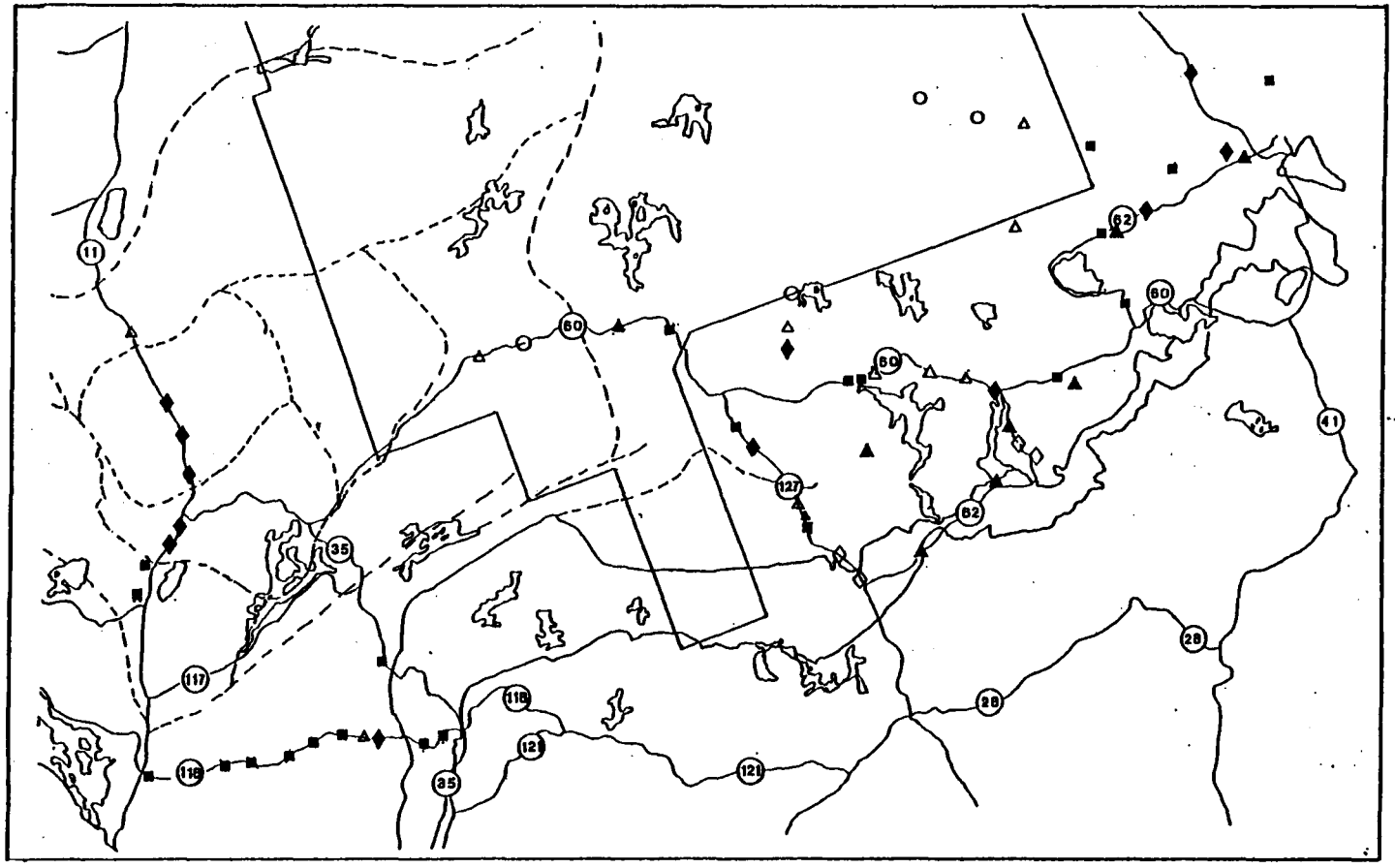

Tdm (Ga)

○ 180–189	■ 150–159
♦ 170–179	▲ 140–149
△ 160–169	◇ 130–139

Table 7.1: Sm/Nd data for the eastern Central Gneiss Belt

nd - not determined

P - Pluton

G - Grey gneiss

S - Paragneiss

Cr, Ba, Al, BB: this study

Mu, Mt: unpublished data

Mr, Ch: Dickin and McNutt, 1991

TABLE 7.1: Sm/Nd data for the Eastern Central Gneiss Belt

Sample	Grid reference	Cor	Qz	*	Nd ppm	Sm ppm	$^{147}Sm/^{144}Nd$	$^{143}Nd/^{144}Nd$	TDM Ga
CARDIFF									
CR5	QV 278973	nd	nd		60.50	8.940	.0893	.512063	1.20
CR8	QA 335091	0.0	4.53	P	nd	nd	nd	nd	nd
BANCROFT									
BA5	TF 713073	1.65	15.29	G?	nd	nd	nd	nd	nd
BA10	TF 687142	1.7	2.60	P?	17.17	3.240	.1141	.512192	1.30
BA11	TF 677153	0.0	9.72	P	nd	nd	nd	nd	nd
BA12	QA 320219	0.76	34.61	G	23.13	5.155	.1347	.512350	1.33
BA13	QA 295268	0.48	15.03	G	29.41	6.296	.1294	.512188	1.54
BA14	QA 287284	0.0	0.0	P	40.78	8.840	.1310	.512247	1.46
BA15	QA 257314	1.49	31.70	S	61.01	10.158	.1005	.5118	1.67
BA16	QA 208360	1.7	37.39	G	39.41	6.905	.1058	.511779	1.78
BA18	QA 196399	0.0	0.0	P	40.47	8.555	.1278	.51216	1.56
BA20	QA 148424	1.2	0.0	P?	26.23	5.193	.1197	.512051	1.61
BA22	QA 109502	0.0	0.0	P?	55.76	11.265	.1221	.512094	1.58
BA23	QA 072519	0.85	0.0	P?	46.20	8.057	.1054	.512024	1.43
BA24	QA 035506	0.0	0.27	P	60.28	12.025	.1207	.51203	1.66
BA25	PA 776415	0.07	0.0	P?	47.44	9.801	.1249	.512085	1.64
BA26	PA 810457	1.30	46.44	S	36.96	5.855	.0957	.511708	1.72
BA27	PA 882473	0.0	10.39	P?	31.45	6.551	.1259	.511969	1.86
BA28	QA 978151	0.0	0.0	P	23.97	5.855	.1251	.512119	1.59
BA36	TF 997020	nd	nd		36.71	8.575	.1412	.512408	1.33
BA37	TF 953038	nd	nd		23.38	3.381	.0874	.512061	1.19
BA38	TF 905153	nd	nd		71.96	11.961	.1005	.512105	1.26
BA39	TF 937201	nd	nd		65.39	17.043	.1576	.512606	1.19
BA40	TF 917338	1.03	0.0	P?	107.09	21.767	.1229	.512215	1.39
BA41	TF 887413	0.0	1.13	P	29.26	5.740	.1186	.511936	1.77
BA42	TF 855423	0.0	6.45	P?	39.56	7.660	.1170	.512009	1.63
BA43	TF 804435	0.58	18.44	G	47.50	8.197	.1041	.511885	1.61
BA44	TF 704454	0.63	13.58	G?	49.12	9.004	.1108	.511946	1.62
BA45	TF 704435	0.0	2.47	P?	46.35	9.464	.1234	.512144	1.51
BA46	QA 272478	0.65	0.0	G?	37.86	7.196	.1149	.511892	1.77
BA47	QA 271484	2.20	23.93	G	29.48	5.953	.1220	.512010	1.71
BA48	QA 265505	1.36	32.16	G	52.73	10.661	.1222	.512081	1.60
BA49	QA 269561	1.85	24.57	G?	62.94	12.933	.1242	.511975	1.82
BA50	TF 668438	0.0	7.36	P?	36.49	7.131	.1181	.512085	1.52
BA51	TF 730392	1.59	19.78	G	31.59	6.189	.1184	.512000	1.67
BA52	TF 709313	0.0	6.94	P	38.78	7.829	.1219	.512144	1.49
ALGONQUIN									
AL1	UF 163755	0.0	9.72	P?	35.48	6.618	.1127	.512036	1.52
AL4	UF 015825	0.01	2.10	P	53.09	8.477	.0965	.511845	1.56
AL5	TF 944854	0.18	8.09	P?	51.07	10.705	.1266	.512114	1.62
AL6	TF 821903	2.61	63.01	S	18.65	4.15	.1345	.512097	1.82
AL9	TF 715945	1.29	31.68	G	18.32	2.847	.0939	.51163	1.80
BARRY'S BAY									
BB2	UF 147661	1.12	25.74	G	22.57	3.971	.1063	.511991	1.49

BB3	UF	057625	0.0	0.0	P?	40.29	7.999	.1200	.512070 1.58
BB5	TF	875632	0.0	0.0	P	48.34	8.662	.1084	.511932 1.61
BB7	TF	974417	0.0	10.3	?	31.44	5.784	.1112	.512035 1.50
BB9	TF	908358	0.0	21.79	G?	32.13	6.87	.1293	.512250 1.43
BB10a	TF	944299	0.0	47.37	S	nd	nd	nd	nd nd
BB15	UF	093535	0.0	0.0	P?	39.72	7.831	.1194	.512069 1.57
BB16	UF	006414	0.0	3.11	P	31.11	6.14	.1193	.512153 1.43
BB17	TF	966312	0.0	21.87	P?	46.52	8.529	.1108	.512112 1.38
BB18	TF	892267	1.73	14.18	G?	28.49	5.770	.1224	.512179 1.44
BB19	TF	858233	0.0	0.0	P?	58.58	10.395	.1073	.512170 1.25
BB20	TF	785178	0.0	6.33	P	33.70	7.555	.1355	.512319 1.41
MUSKOKA									
MU1	PV	353832	0.61	24.07	G	39.80	7.120	.1081	.511956 1.57
MU10	PV	806902							
MU11	PV	532843	0.84	17.41	G	81.78	14.290	.1056	.511980 1.50
MU2	PV	433838	0.0	12.60	G	30.04	5.621	.1131	.512014 1.56
MU3	PV	437842	6.09	13.44	S	32.55	5.598	.1040	.511909 1.57
MU4	PV	475850	0.0	6.18	P	36.81	7.290	.1197	.512059 1.59
MU5	PV	578875	0.0	2.46	P	48.46	10.390	.1295	.512118 1.67
MU6	PV	619895	0.98	27.69	G	29.50	6.300	.1297	.512221 1.49
MU7	PV	647887	0.0	10.86	P?	66.15	13.87	.1267	.512068 1.70
CH4			0.0	4.38	P	54.00	10.442	.1169	.511953 1.71
CH2	PV	706992	0.0	4.31	P	45.29	8.375	.1119	.512008 1.55
CH3			0.0	4.85	P	33.50	5.950	.1074	.511839 1.72
HUNTSVILLE									
MR164.4	PA	291467	1.24	28.42	G				1.64
MR177.2	PA	358361	1.08	35.04	G	23.49	3.716	.0956	.511681 1.76
MR187.3	PA	389269	0.68	25.24	G	27.29	4.823	.1074	.511848 1.71
MR192	PA	386228	0.0	6.75	P	46.53	8.999	.1169	.511984 1.66
MR198.4	PA	363170	2.62	30.95	G	43.62	7.745	.1074	.511846 1.71
MR199.8	PA	355158	0.0	0.44	P	36.70	7.653	.1259	.512025 1.76
MR202.2	PA	343139	0.48	22.88	G?	30.78	5.825	.1144	.512033 1.55
MR207.1	PA	327093	0.82	6.14	P	42.03	8.179	.1176	.512059 1.56
MR214.7	PA	327017	0.0	0.0	P	45.11	9.866	.1322	.512174 1.62
MR242.5	PV	310776	0.0	11.29	P	17.93	3.727	.1255	.512149 1.54
MR176.4	PA	353369	1.42	39.52	G	47.12	8.758	.1124	.511901 1.72
OTTAWA RIVER									
MT15			1.08	46.15	S				
MT18	UF	256781	1.33	35.12	G?				
MT19	UF	293730	0.06	14.74	G	9.15	1.335	.0881	.511867 1.43
MT22	UF	355875	1.14	22.21	G				
MT23	UF	318897	0.79	22.66	G	23.27	3.960	.1029	.511 1.51

Fig. 7.2: Histogram of model ages for all samples. The large number of samples with a 1.50 to 1.60 Ga model age suggests that this time bracket represents a real geological event.

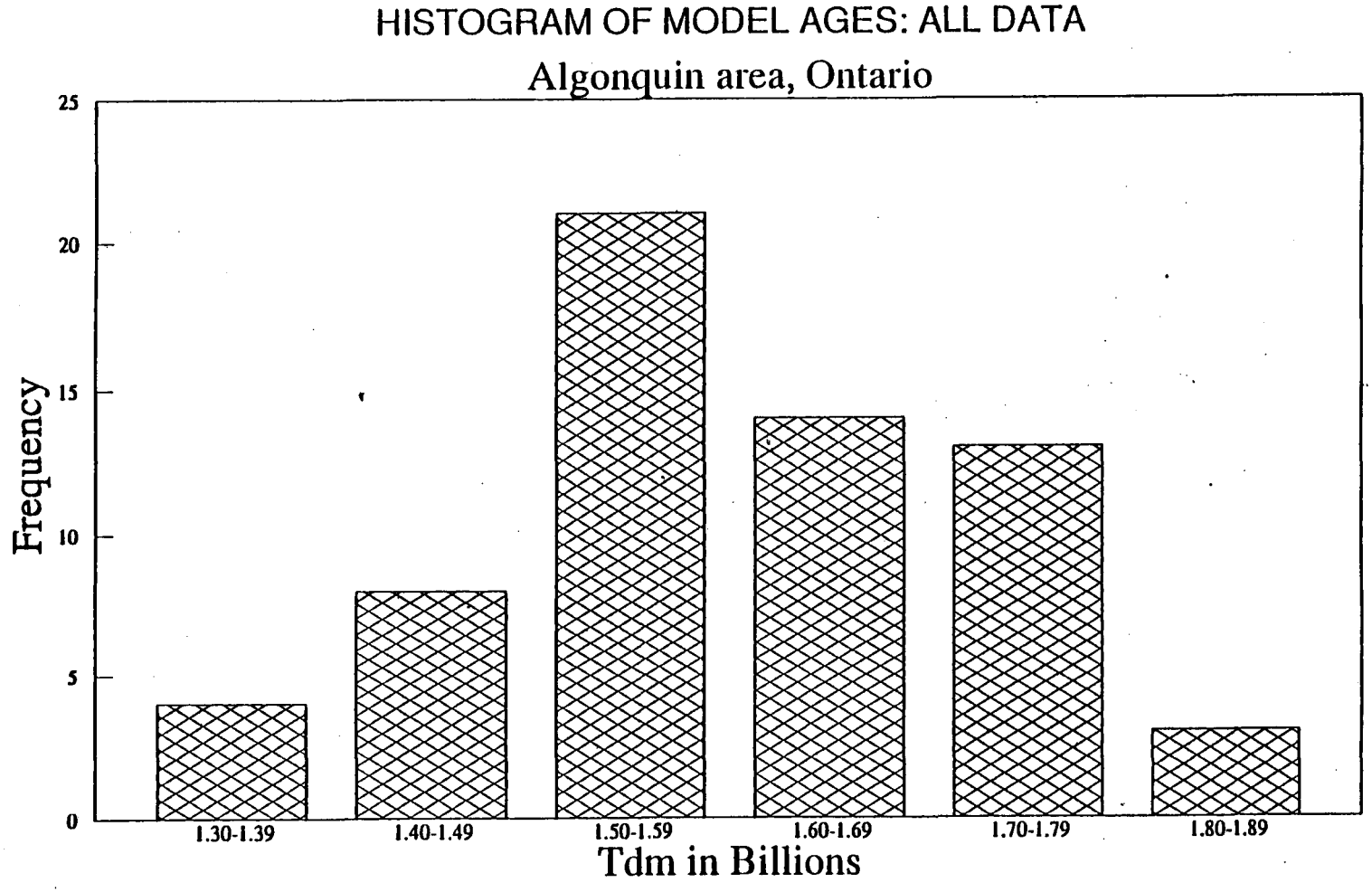
HISTOGRAM OF MODEL AGES: ALL DATA
Algonquin area, Ontario
Frequency
25
20
15
10
5
0
1.30-1.39
1.40-1.49
1.50-1.59
1.60-1.69
1.70-1.79
1.80-1.89
Tdm in Billions

difficult on a hand specimen level. Therefore, major element analysis was done using XRF. A summary of the selected major element analyses is shown in the appendix.

From the CIPW normalized data, the rocks were divided into three main groups: orthogneisses, paragneisses, and gray gneisses. The orthogneisses were identified by their low normative quartz and corundum and high diopside. The paragneisses were identified by their high normative quartz and corundum and low diopside. The gray gneisses were identified by their intermediate compositions. Of the seventy samples that were in and around the field area, thirty-one are thought to represent orthogneisses, twenty-five are thought to represent gray gneisses, and 5 were thought to represent paragneisses. The remaining nine were difficult to assign a provenance to. From the summary histogram of all data, the large peak between 1.50 and 1.60 Ga suggests that there may have been an actual geological event during this time period. This is best exemplified by the large number of recognizable plutons contained in this age bracket as shown in Figure 7.3.

In order to determine if there was any spatial-temporal trends, the data were plotted on a graph of model age vs. distance from the CMBBZ (Fig. 7.4). The graph suggests that samples younger than 1.50 Ga may represent a separate terrane. However, rocks older than 1.50 Ga occur at variable distances from the CMBBZ. To better resolve what

Fig. 7.3: Histogram of orthogneisses as identified from low normative quartz and corundum and high normative diopside. Suggests that most activity occurred between 1.50 and 1.60 Ga ago.

HISTOGRAM OF PLUTONS

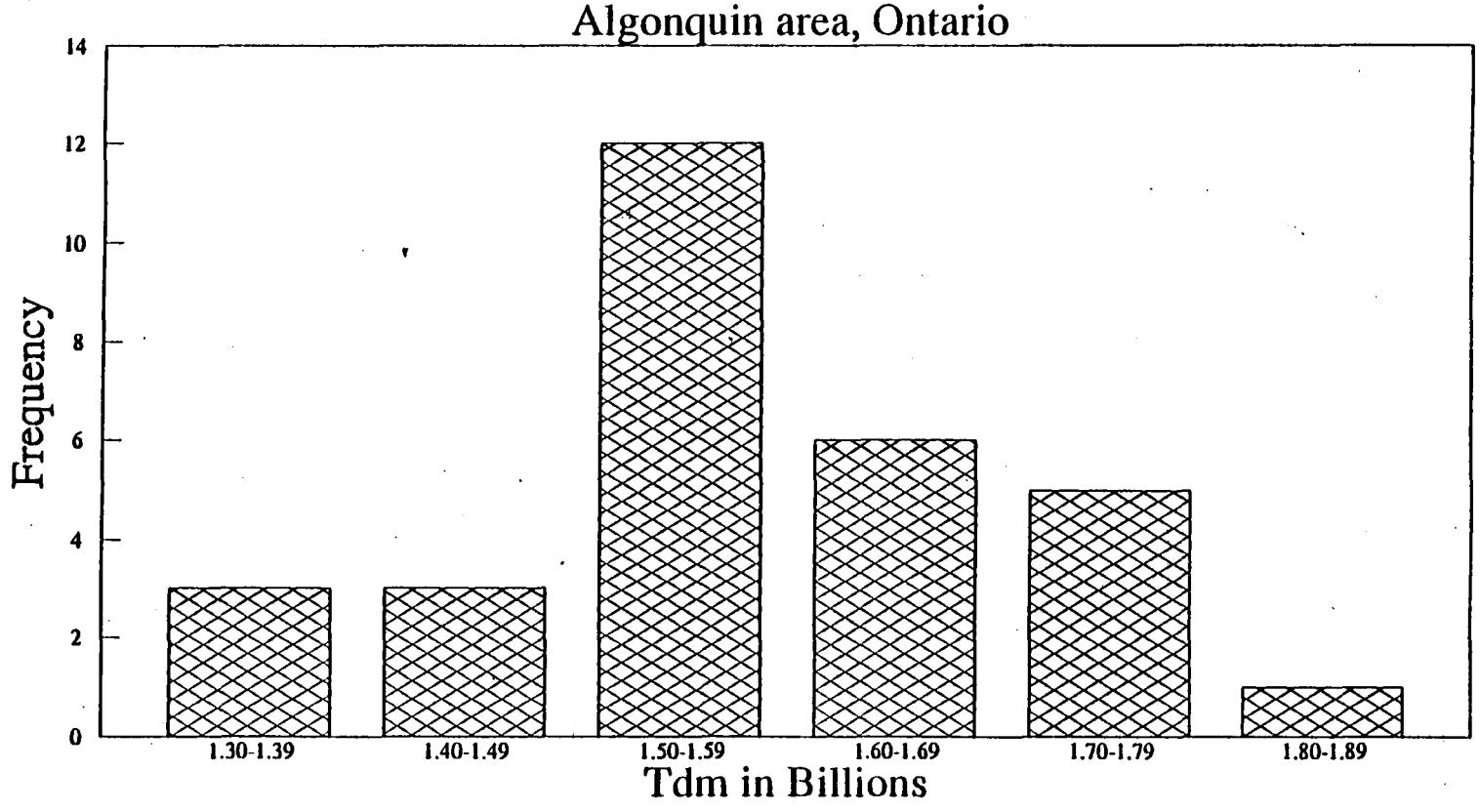

Fig. 7.4: Plot of model age vs. distance from the CMBBZ. Two fields can be recognized: For rocks younger than 1.50 Ga, there is a tight cluster within 15 km north of the CMBBZ, suggesting that these rocks may represent a separate terrane. Rocks older than 1.50 Ga occur at variable distances from the CMBBZ implying a mixing model of older and younger components.

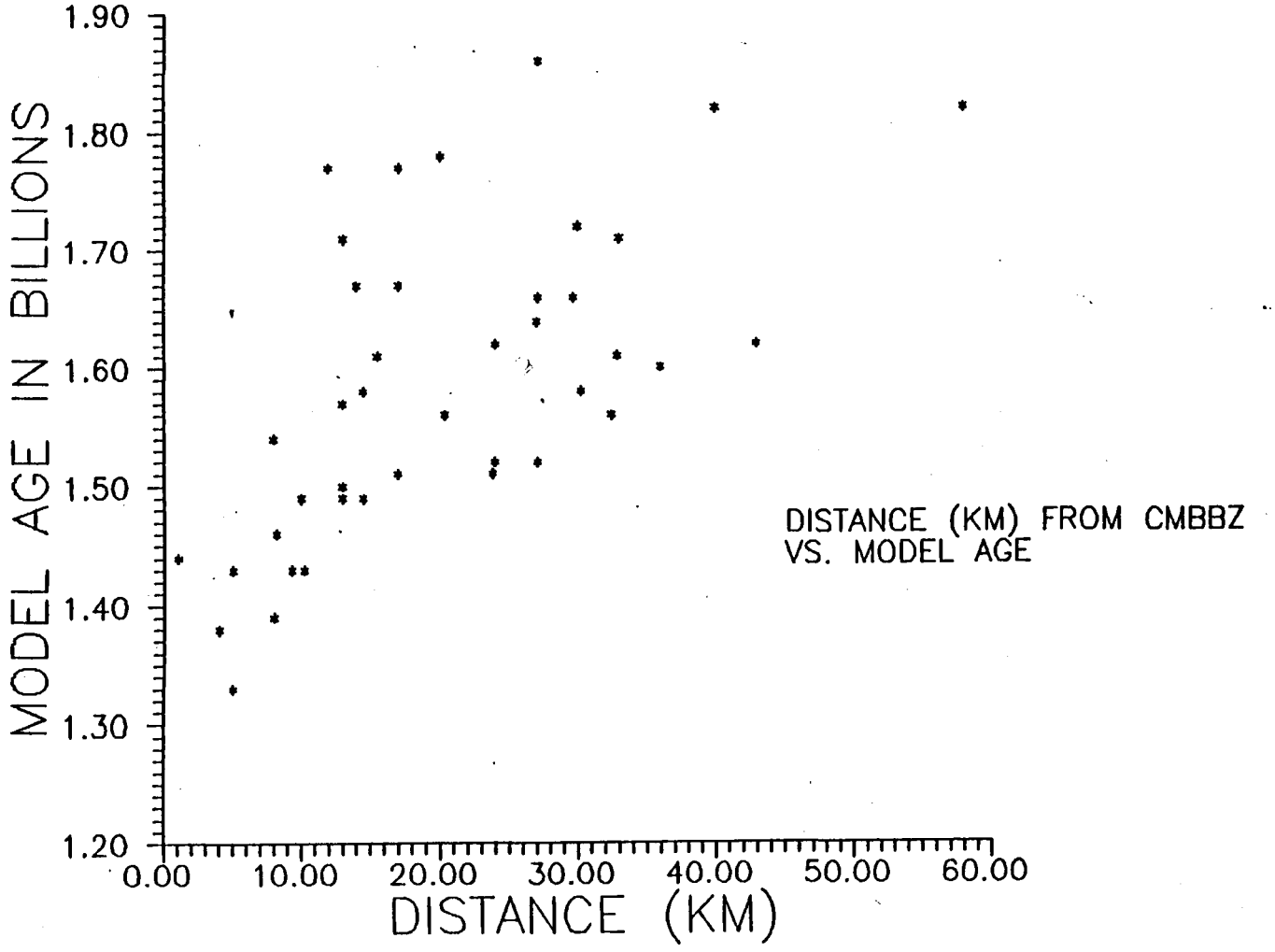
MODEL AGE IN BILLIONS
1.90
1.80
1.70
1.60
1.50
1.40
1.30
1.20
0.00
10.00
20.00
30.00
40.00
50.00
60.00
DISTANCE (KM)
DISTANCE (KM) FROM CMBBZ
VS. MODEL AGE

tectonic environments these rocks may represent, two different petrological discrimination diagrams have been used.

The first diagram is an AFM plot (Fig. 7.5). The weight percent oxides were plotted for all seventy samples in and around the field area. The younger samples south of the CMBBZ were excluded. The area outlined represents the Blanco Batholith of Peru (Atherton and Sanderson, 1987). The majority of samples lie within the calc-alkaline field defined by the Blanco Batholith. Of the twelve samples located outside of the calc-alkaline trend, six represent paragneisses and six represent mafic orthogneisses. The paragneissic samples represent re-worked material and thus would not be expected to lie within the calc-alkaline field, unless they were composed of juvenile calc-alkaline sediments. However, the older model ages for these paragneissic samples suggests that they are composed of older sediments. The six mafic plutons lying outside of the calc-alkaline field probably represent anorogenic plutonism that occurred at various times as indicated by their wide range of model ages.

The second petrological discrimination diagram used was developed by LeFort and Debon (1983) (Fig. 7.6). The diagram uses the two co-ordinates Q and P as shown, expressed as gram-atoms x 10^3. The field outlined to the right represents anorogenic plutons analyzed by Dickin et al., (1990) while the field across the top represents gray

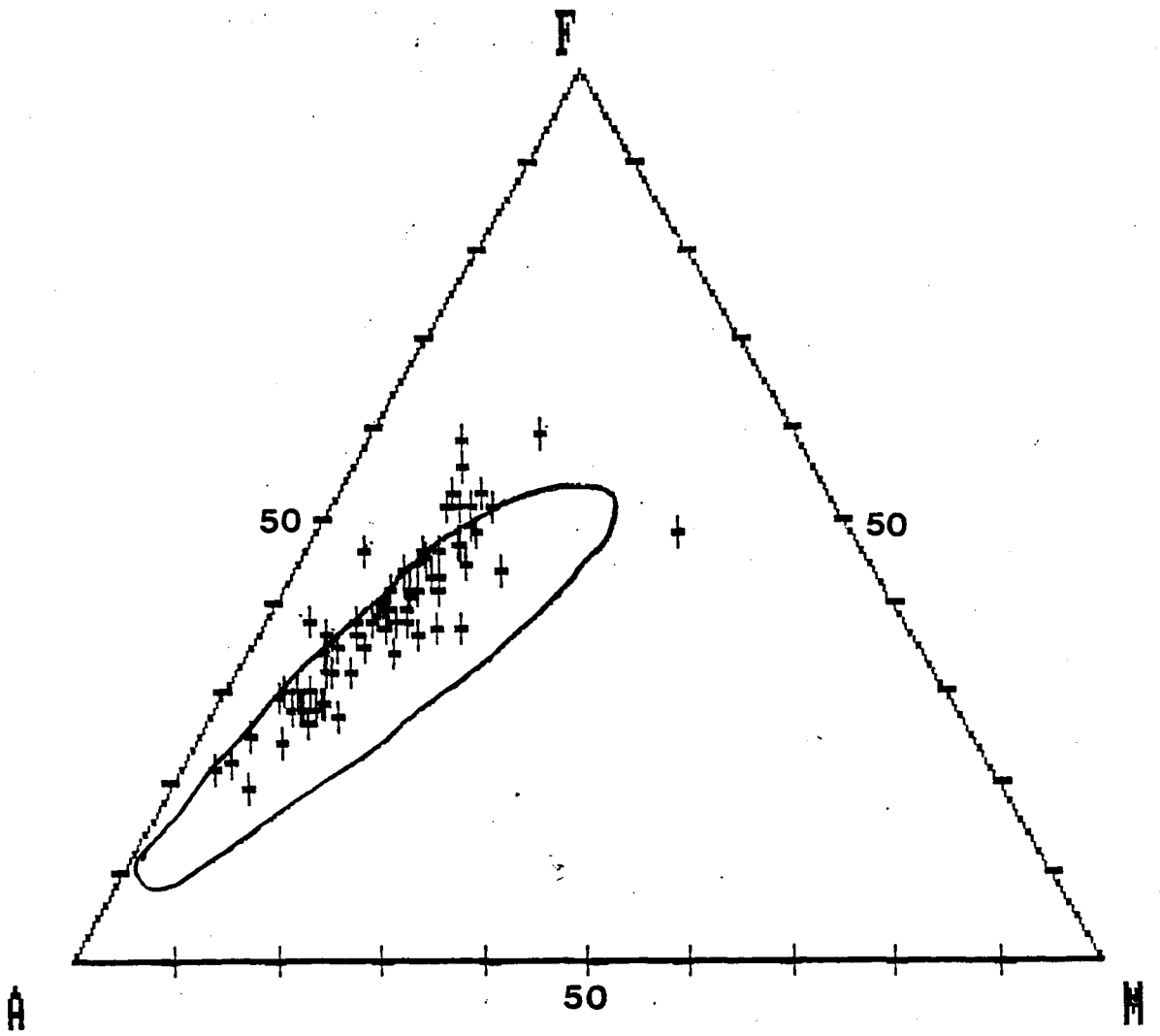

Fig. 7.5: AFM diagram of all samples analyzed from the Algonquin Park area. Field outlined is that of the Blanco Batholith of Peru. The majority of samples fall within this calc-alkaline field, suggesting that the Algonquin Park area represents a continental margin ensialic arc just as the Blanco Batholith does. (A = wt. % oxides of Na + K, F = wt. % FeO + Fe_2O_3, M = wt. % MgO).

Fig. 7.6: Granitoid discrimination diagram of LeFort and Debon (1983). The field outlined on the right represents anorogenic plutons analyzed by Dickin et al., (1990). The field outlined across the top represents orogenic gray gneisses analyzed by Dickin and Higgins, (1992). Most samples lie between these two fields suggesting that the rocks are composed of orogenic and anorogenic components. to = tonalite, gd = granodiorite, ad = adamellite, gr = granite, qd = quartz diorite, qmd = quartz monzodiorite, qm = quartz monzonite, go = gabbro, mgo = monzogabbro, mo = monzonite.

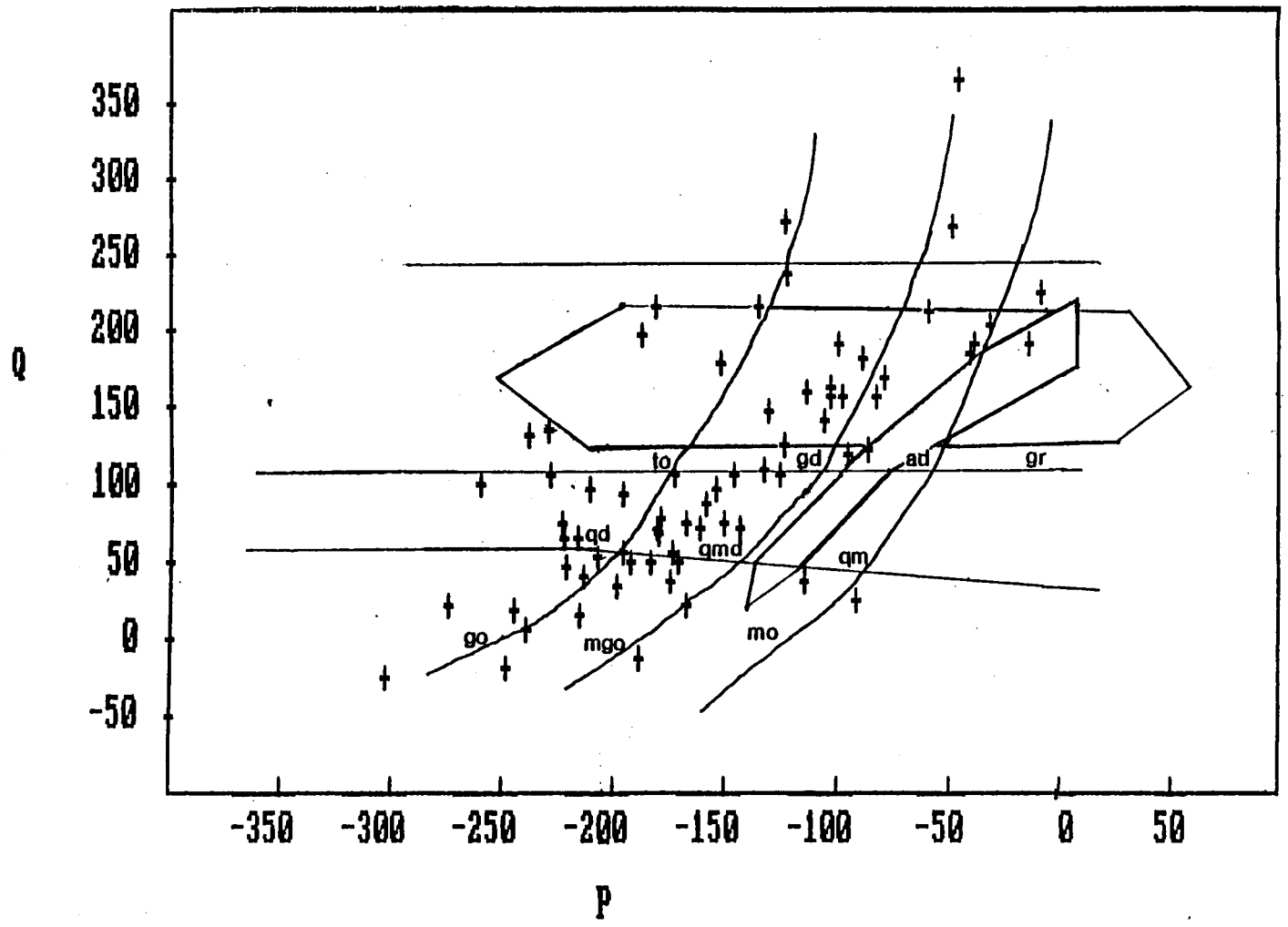

$$Q = {}^{Si}/_{3} - (K + Na + 2{}^{Ca}/_{3})$$

$$P = K - (Na + Ca)$$

gneisses thought to exemplify orogenic island arc rocks analyzed by Dickin and Higgins (1992). The majority of the samples from the field area seem to lie between these two fields, suggesting an intermediate type of process as might be expected for an ensialic continental margin arc.

A similar variety of lithologies are present in the Peruvian Batholith. For example, a Quartz - Alkali feldspar - Plagioclase (QAP) diagram for the Lima and Arequipa segments of the Peruvian Batholith reveal the same trend of intermediate compositions (Figure 7.7, Atherton et al., 1979).

7.1.1 ZIRCON DATING

The results of Pb-Pb zircon dating by direct evaporation are shown in Fig. 7.8. The zircons were extracted from sample BA15 whose Nd model age was determined as 1670 +/- 20 Ma (2o). Using the major element analyses, the sample falls into the category of a gray gneiss. However, when plotted on the discrimination diagram of LeFort and Debon (1983), the sample lies within the granite field, indicating that this sample represents an orthogneiss. Of the thirty-five zircons extracted from BA15, only seven produced usable data.

The zircon data show a very wide range of ages from 1635 Ma to 1210 Ma. The younger zircon ages likely represent Pb loss from 1635 zircons because this sample was obtained from a granulite grade rock. Because the oldest zircon age and the

Fig. 7.7: QAP diagram for the Lima (closed circles) and Arequipa (open circles) segments of the Peruvian Coastal Batholith. The mix of lithologies in the Coastal Batholith are similar to those found in the Algonquin Park area as revealed by the granitoid discrimination diagram of LeFort and Debon (1983) (after Atherton et al., 1979).

1. Quartzolite 2. Tonalite 3. Quartz diorite/ Quartz gabbro/ quartz anorthosite 4. Diorite/ Gabbro/ Anorthosite 5. Granodiorite 6. Quartz monzodiorite/ Quartz monzogabbro 7. Monzodiorite/ Monzogabbro

8. Granite 9. Quartz monzonite 10. Monzonite

11. Granite 12. Quartz syenite 13. Syenite

14. Alkali feldspar granite 15. Alkali feldspar quartz syenite 16. Alkali feldspar syenite

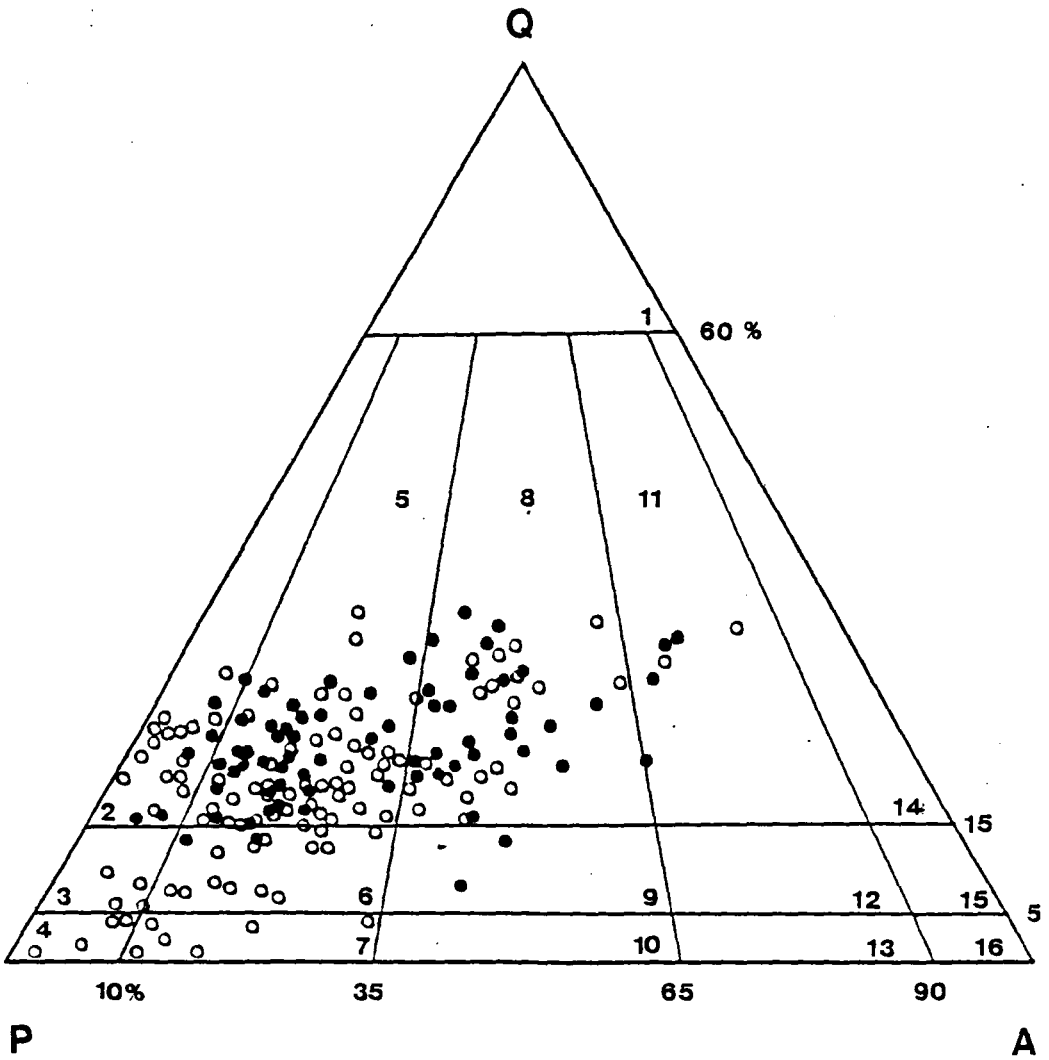
Q
1
60 %
5
8
11
2
14
15
3
6
9
12
15
5
4
7
10
13
16
10%
35
65
90
P
A

Fig. 7.8: Plot of $^{207}Pb/^{206}Pb$ vs. $^{204}Pb/^{206}Pb$ for zircons extracted from granulite grade orthogneiss BA15. The wide range of ages is likely a result of Pb loss. The oldest zircon is within error of the model age determined for BA15, suggesting that 1635 Ma is the crystallization age for this pluton. The zircon dates were determined from two point isochrons between zircon data and their respective common Pb concentrations calculated using Stacey and Kramers (1975) estimation of terrestrial Pb.

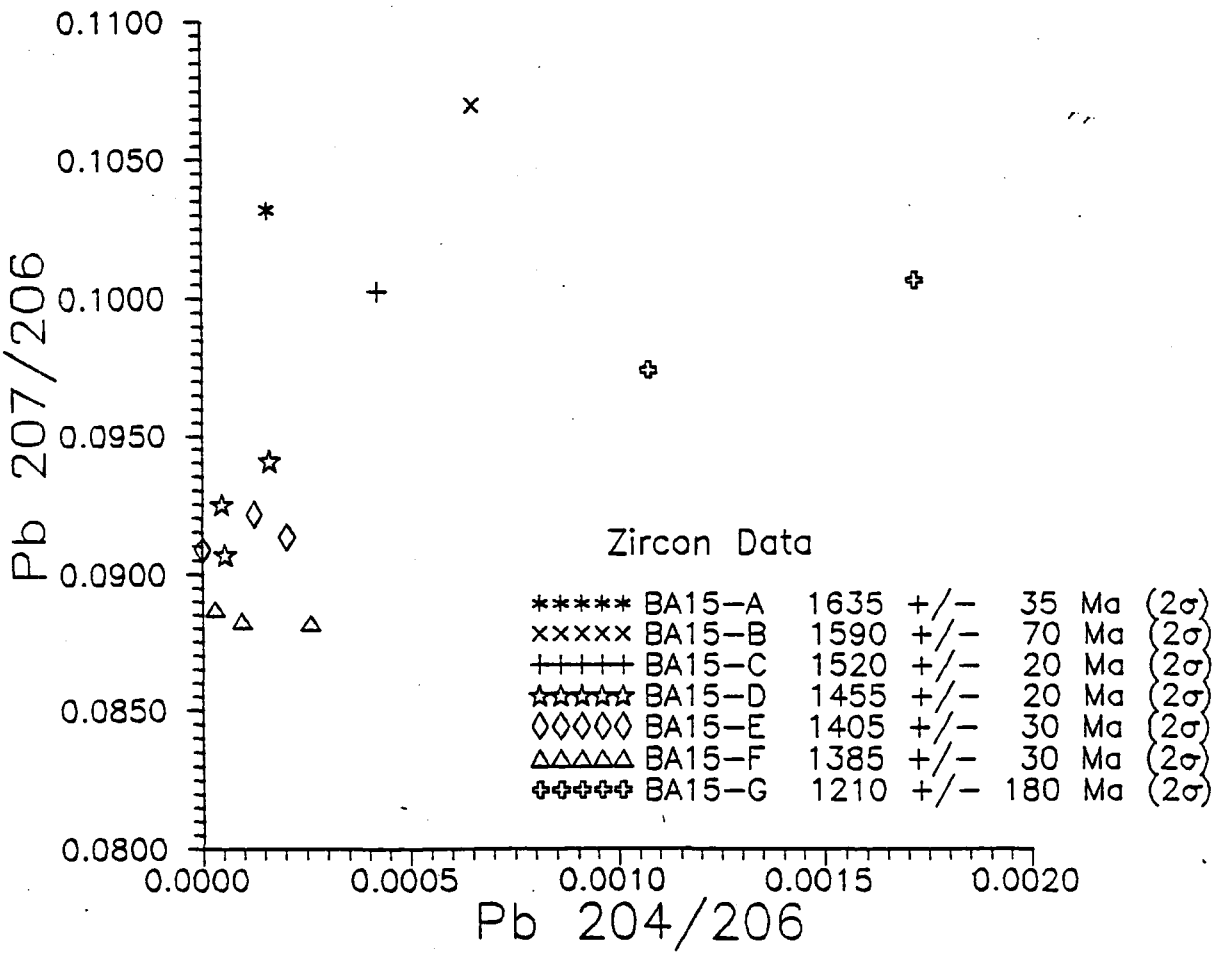
0.1100
0.1050
0.1000
0.0950
0.0900
0.0850
0.0800
Pb 207/206
0.0000
0.0005
0.0010
0.0015
0.0020
Pb 204/206
Zircon Data
***** BA15–A 1635 +/– 35 Ma (2σ)
xxxxx BA15–B 1590 +/– 70 Ma (2σ)
+++++ BA15–C 1520 +/– 20 Ma (2σ)
☆☆☆☆☆ BA15–D 1455 +/– 20 Ma (2σ)
◊◊◊◊◊ BA15–E 1405 +/– 30 Ma (2σ)
△△△△△ BA15–F 1385 +/– 30 Ma (2σ)
✣✣✣✣✣ BA15–G 1210 +/– 180 Ma (2σ)

model age for this sample are within error, the 1635 age likely represents the approximate crystallization age for this orthogneiss.

CHAPTER 8

DISCUSSION AND CONCLUSIONS

The separate lines of evidence described above suggest that the Algonquin Park area in the Central Gneiss Belt of the southwestern Grenville Province in Ontario may represent an ensialic continental margin arc that was active between 1.50 and 1.60 Ga ago. This conclusion is derived from three independent sources. Firstly, the rocks in the Algonquin area north of the CMBBZ have a clear cut calc-alkaline signature as illustrated by the AFM diagram. Virtually all of the samples lie within the field defined by a modern version of an ensialic continental margin arc: the Blanco Batholith of Peru. Any samples that do not lie within this calc-alkaline trend are either paragneisses or gabbroic plutons. The paragneissic samples are not composed strictly of juvenile calc-alkaline sediments. This is illustrated by the older model ages for these paragneisses, implying that there are substantial volumes of older sediment present. Thus, the paragneiss locations on the AFM plot have little relevance with regards to whether or not the Algonquin area represents an ensialic continental margin arc.

The second line of evidence is derived from the granitoid discrimination diagram of LeFort and Debon (1983). The

field in which the rocks of the Algonquin Park area fall is intermediate between orogenic rocks and anorogenic rocks. This suggests that the rocks in the Algonquin Park area illustrate variable mixing of an older crustal component, represented by the existing continental margin rocks, and a juvenile, orogenic component, produced by the subducting oceanic slab beneath the continental margin. The diapiric rise of plutons formed in this subduction zone incorporated some of the existing anorogenic country rocks and hence changed their apparent provenance geochemical signatures from tonalitic and granodioritic typical of continental arcs, to monzogabbro and quartzmonzodiorite.

The third line of evidence arises from the wide temporal and spatial range of model ages determined for the rocks in the Algonquin Park area. Except for a small segment immediately north of the CMBBZ in the eastern part of the field area, the majority of the rocks in this portion of the Central Gneiss Belt show no major step-wise changes in model age. The wide range of model ages between ten and sixty km north of the CMBBZ suggests that the rising plutons developed in this 1.60 to 1.50 Ga old subduction zone incorporated variable amounts of existing country rocks, thereby yielding mixed model age signatures for the plutons. The different rising plutons assimilated variable amounts of existing continental margin. Some plutons incorporated very little

country rock. This is supported by the close agreement between the Pb-Pb zircon ages and the model age calculated for the same sample. Perhaps sufficient continental underplating had developed so as to "force" some plutons through thicker portions of continental crust. These plutons would assimilate larger volumes of existing continental rocks and thus produce older model ages.

The reason why some plutons undergo more mixing than other plutons is not known. However, the degree of mixing may be linked to the angle of the subducting oceanic slab and the resulting increase in heat flow and tensional forces that would develop. For example, with a low subduction angle, the heat flow and tensional stresses would be higher and would affect a larger area. Plutons developed during a low angle subduction would have less time to assimilate country rock because melting would occur stratigraphically higher. The increased tensional forces would produce a superior conduit system for the rising magma. The net result for these plutons would be a younger average model age over a large area because there would be less chance of country rock assimilation. Similarly, a steep subduction angle would permit rising plutons to incorporate more country rock. These plutons would have an older average model age. However, the causes for subduction angle changes are not known. Perhaps a change in plate velocity could be attributed to the change in subduction

angle. Further study of modern analogues is required before such conclusions can be proven.

The area of rocks with model ages younger than 1.50 Ga, located immediately north of the CMBBZ show a fairly sharp truncation with the older rocks further north. Perhaps this area represents a 1.45 Ga island arc terrane that was "piggy-backed" by the subducting slab and eventually sutured onto the continental margin. The southern portion of the island arc was later overridden by the northwestward directed ductile thrusting of the Grenville event 300 to 400 Ma later. However, further work must be done on this area in order to justify this.

The suggestion that the Algonquin area represents an ancient subduction zone is not restricted to the Central Gneiss Belt of Ontario. For example, in the Lac St. Jean area of Quebec, Dickin and Higgins (1992) have discovered a 1.53 Ga island arc that was accreted to the continental margin. Although the time of accretion is not known, the island arc was thought to have sutured to the North American craton soon after its extraction from the mantle.

Thus, in conclusion, the evidence suggests that the Algonquin Park area in the Central Gneiss Belt in the southwestern portion of the Grenville Province of Ontario may represent an ensialic continental margin arc that was active between 1.50 and 1.70 Ga ago. A cartoon representing a

possible tectonic model is shown in Fig. 8.1. There are three main stages. The early stage represents the start of subduction approximately 1.65 Ga ago. The rising plutons intruded continental margin arcs at least as old as 1.86 Ga illustrated by the pluton with the oldest model age in the field area. Plutonism continued for at least 150 Ma. The middle stage represents continued continental plutonism and the formation and transportation of a mid Proterozoic island arc. The final stage represents collision of the island arc with the continental margin. Plutonism continued, as illustrated by the younger model ages obtained from within and to the south of the CMBBZ.

Although the evidence to date suggests that this subduction zone did exist, further trace element analysis must be done in order to strengthen this contention. For instance, determination of Nb, Ta, and Ti depletions in the Algonquin area rocks would further indicate the presence of the intrusive equivalents of volcanic arc rocks typical of a continental-oceanic subduction zone. More samples within the zone thought to represent an accreted island arc must be analyzed before such conclusions can be proven. Zircon dating must also be done on paragneissic samples so as to better establish the theory of mixed provenance sediments producing mixed model ages.

Fig. 8.1: Tectonic model for the Algonquin area.
First stage (1.50-1.65 Ga): plutons formed at subduction zone intrude existing continental margin at least as old as 1.86 Ga (oldest pluton in area), producing an ensialic continental margin arc.
Second stage (1.40-1.50 Ga): Subduction continues, transporting an island arc approximately 1.45 Ga towards the continental margin.
Third stage: The island arc collides with the continental margin at an unknown time. Plutonism continues.

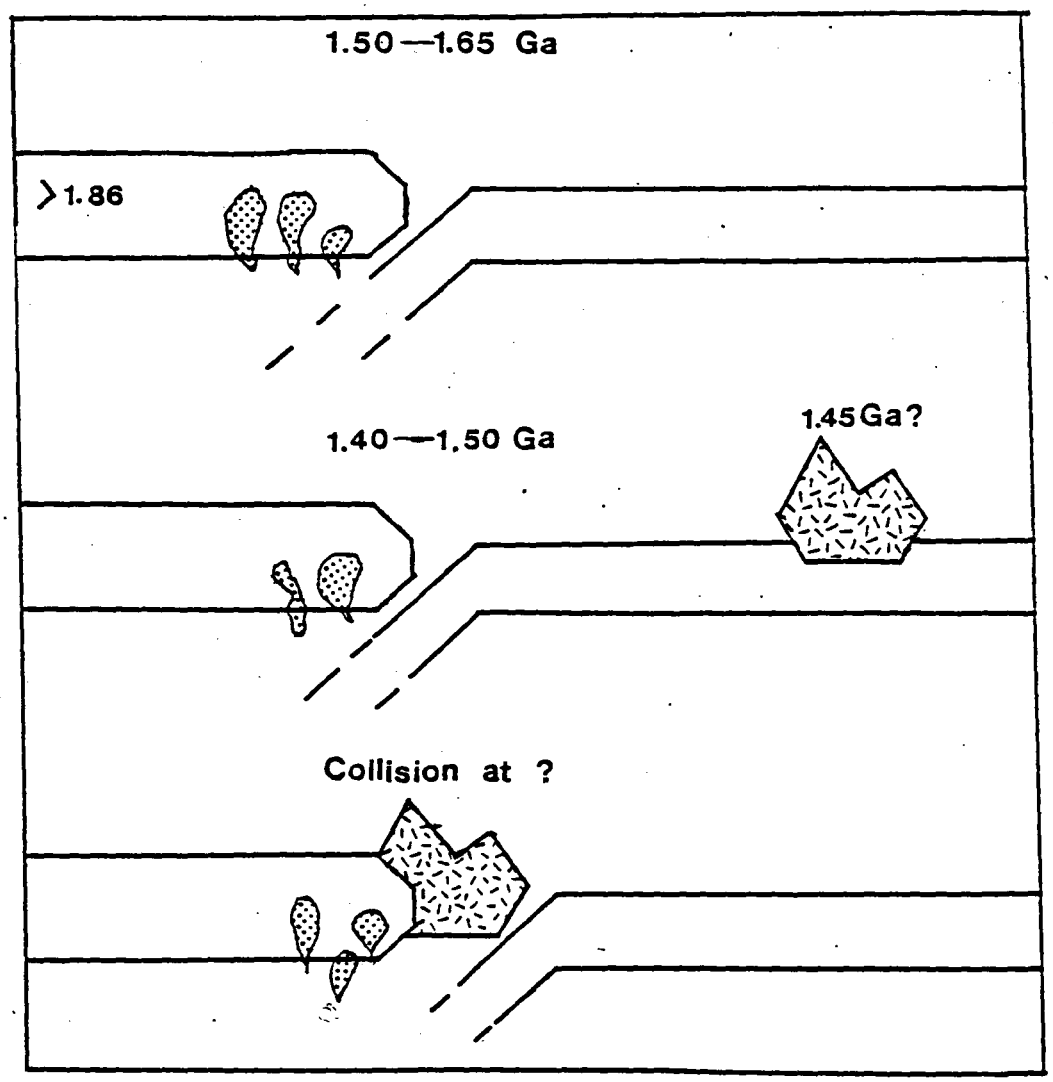
1.50—1.65 Ga
>1.86
1.40—1.50 Ga
1.45Ga?
Collision at ?

References

Arndt, N.T., Goldstein, S.L., 1987, Use and abuse of crust-formation ages: Geology, v. 15, p. 893-895.

Atherton, M.P., and Sanderson, L.M., 1987, The Cordillera Blanca Batholith: a study of granite intrusion and the relation of crustal thickening to peraluminosity: Geologische Rundschau, v. 76, p. 213-232.

Atherton, M.P., McCourt, W.J., Sanderson, L.M., and Taylor, W.P., 1979, The geochemical character of the segmented Peruvian Coastal Batholith and associated volcanics, in Atherton, M.P., and Tarney, J., eds., Origin of Granite Batholiths: Geochemical Evidence

Culshaw, N.G., Davidson, A., and Nadeau, L., 1983, Structural subdivisions of the Grenville Province in the Parry Sound-Algonquin region, Ontario; in Current Research, Part B, Geological Survey of Canada, Paper 83-1B, p. 243-252.

Davidson, A., 1986, New interpretations in the southwestern Grenville Province, in Moore, J.M., Davidson, A., Baer, A.J., eds., The Grenville Province: Geological Association of Canada Special Paper #31, p. 61-74.

Davidson, A., and Grant, S.M., 1986, Reconnaissance geology of western and central Algonquin Park and detailed study of coronitic olivine metagabbro, Central Gneiss Belt, Grenville Province of Ontario, in Current Research, Part B, Geological Survey of Canada, Paper 86-1B, p. 837-848.

DePaolo, D.J., 1981a, Nd isotopic studies: Some new perspectives on Earth structure and evolution: EOS v. 62, p. 137-140.

DePaolo, D.J., 1981c, Neodymium isotopes in the Colarado Front Range and crust-mantle evolution in the Proterozoic: Nature, v. 291, p. 193-196.

DePaolo, D.J., 1988, Neodymium Isotope Geochemistry: an Introduction, Springer-Verlag, Germany, pp. 187.

Dickin, A.P., and McNutt, R.H., 1989, Nd model age mapping of the southeast margin of the Archean foreland in the Grenville Province of Ontario: Geology, v.17, p. 299-302.

Dickin, A.P., McNutt, R.H., and Clifford, P.M., 1990, A neodymium isotope study of plutons near the Grenville Front in Ontario: Chemical Geology, v. 83, p. 315-324.

Dickin, A.P., and McNutt, R.H., 1991, Nd model-age mapping of Grenville Lithotectonic domains: Mid-Proterozoic crustal evolution in Ontario in Gower, C.F., Rivers, T., and

Ryan, B., eds., Mid-Proterozoic Laurentia-Baltica: Geological Association of Canada, Special Paper #38, p. 79-94.

Dickin, A.P., and Higgins, M.D., 1992, Sm/Nd evidence for a major 1.5 Ga crust-forming event in the central Grenville province: Geology, v. 20, p. 137-140.

Easton, R.M., 1986, Geochronology of the Grenville Province in Moore, J.M., Davidson, A., Baer, A.J., eds., The Grenville Province: Geological Association of Canada Special Paper #31, p. 127-173.

Grossman, L., and Larimer, J.W., 1974, Early chemical history of the solar system: Rev. Geophys. Space Phys., v. 12, p. 71-101.

Hamner, S., 1988, Ductile thrusting at mid-crustal level, southwestern Grenville Province: Can. J. Earth Sci., v. 25, p. 1049-1059.

Holmden, C., 1990, Early Proterzoic evolution of the Grenville belt: Evidence from Nd isotopic mapping, North Bay, Ontario, unpublished B.Sc. Thesis, McMaster University, Hamilton, Ontario. pp. 76.

LeFort, P., and Debon, F., 1983, A chemical-mineralogical classification of common plutonic rocks and associations: Royal Society of Edinburgh Transactions, Earth Sciences,

v. 73, p. 135-149.

Moore, J.M., Introduction: The "Grenville Problem", then and now, 1986, in Moore, J.M., Davidson, A., and Baer, A.J., eds., 1986, The Grenville Province: Geological Association of Canada Special Paper #31, p. 1-11.

Mueller, E.L., 1991, Pb-Pb zircon dating by direct evaporation: Method development and selected geological applications, unpublished M.Sc. Thesis, McMaster University, Hamilton, Ontario, pp. 158.

Nelson, B.K., and DePaolo, D.J., 1985, Rapid production of continental crust 1.7-1.9 b.y. ago: Nd isotope evidence from the basement of the North American mid-continent: Geological Society of America Bulletin, v. 96, p. 746-754.

Rivers, T., Martignole, J., Gower, C.F., and Davidson, A., 1989, New tectonic divisions of the Grenville Province, southeast Canadian Shield: Tectonics, v. 8, no. 1, p. 63-84.

Schwerdtner, W.M., and Lumbers, S.B., 1980, Major diapiric structures in the Superior and Grenville provinces of the Canadian Shield; in The Continental Crust and its Mineral Deposits, ed. D.M. Strangway: Geological Association of Canada Special Paper #20, p. 149-180.

Stacey, J.S., and Kramers, J.D., 1975, Approximation of terrestrial lead isotope evolution by a two-stage model: Earth Planet. Sci. Lett., v. 26, p.207-221.

Stockwell, C.H., 1964, Fourth report on structural provinces, orogenies, and time classification of rocks of the Precambrian Shield in Age determinations and Geological Studies: Geological Survey of Canada Paper 64-17 (part 2), p. 1-21.

Thirlwall, M.F., 1982, Atriple filament method for rapid and precise analysis of rare-earth elements by isotope dilution: Chemical Geology, v. 35, p. 155-166.

van Breemen, O., Davidson, A., Loveridge, W.D., and Sullivan, R.W., 1986, U/Pb zircon goechronolgy of Grenville tectonites, granulites and igneous precursors, Parry Sound, Ontario in Morre, J.M., Davidson, A., Baer, A.J., eds., The Grenville Province: Geological Association of Canada Special Paper #31, p. 191-207.

Wynne-Edwards, H.R., 1972, The Grenville Province, in Price, R.A., and Douglas, R.J.W., eds., Variations in tectonic styles in Canada: Geological Association of Canada Special Paper #11, p. 263-334.

York,D., 1969, Least squares fitting of a straight line with correlated errors: Earth Planet. Sci. Lett., v. 5, p.

320 - 324.

APPENDIX : TABLE OF MAJOR ELEMENT ANALYSES

nd - NOT DETERMINED

Ap - APATITE

Il - ILMENITE

Mt - MAGNETITE

Or - ORTHOCLASE

Ab - ALBITE

An - ANORTHITE

Di - DIOPSIDE

Hy - HYPERSTHENE

Ol - OLIVINE

Ne - NEPHELINE

C - CORUNDUM

Q - QUARTZ

A - Na & K OXIDES

M - Mg OXIDES

F - Fe OXIDES

Q - Q OF LeFORT & DEBON, 1983

P - P OF LeFORT & DEBON, 1983

	MR164	MR177	MR187	MR192	MR198	MR199	MR202	MR207	MR214	MR242
SIO2	65.06	68.53	64.89	54.83	66.47	51.01	62.23	54.00	52.04	56.31
TIO2	0.36	0.16	0.33	0.53	0.30	0.68	0.37	0.86	0.58	0.36
AL203	16.21	15.39	16.66	19.76	16.86	20.65	17.32	21.24	21.00	18.13
FE203	0.32	0.17	0.23	0.48	0.19	0.61	0.33	0.43	0.46	0.45
FEO	3.56	1.88	2.56	5.32	2.11	6.76	3.62	4.74	5.13	4.99
MNO	0.02	0.04	0.05	0.09	0.04	0.09	0.06	0.08	0.07	0.07
MGO	1.97	1.74	1.38	2.98	1.59	3.44	2.44	2.28	3.38	4.46
CAO	2.59	2.39	2.40	5.18	1.84	6.93	3.70	5.01	5.41	5.95
NA20	4.77	7.41	7.67	7.69	5.44	7.17	5.37	8.05	9.01	6.40
K20	5.10	2.25	3.75	2.98	5.11	2.55	4.45	3.09	2.70	2.75
H20+	nd	nd	nd	nd	nd	nd	nd	nd	nd	nd
H20-	nd	nd	nd	nd	nd	nd	nd	nd	nd	nd
P205	0.04	0.06	0.08	0.16	0.05	0.13	0.12	0.23	0.22	0.13
TOTAL	100.00	100.00	100.00	100.00	100.00	100.00	100.00	100.00	100.00	100.00
Ap	.11600	.15917	.22843	.50033	.13643	.38537	.34962	.68143	.65874	.38016
Il	1.02	.45259	.92911	1.59	.84611	2.02	1.07	2.52	1.73	1.07
Mt	.69268	.36199	.49644	1.08	.40552	1.39	.71131	.95302	1.04	1.01
Or	26.41	11.54	19.38	16.18	26.13	13.97	23.34	16.59	14.59	14.80
Ab	23.29	35.85	37.43	39.40	26.23	36.96	26.53	40.67	45.96	32.44
An	13.05	11.78	11.74	24.70	9.03	29.93	18.36	24.84	25.16	24.19
Di	nd	nd	nd	1.62	nd	5.62	nd	nd	1.80	5.62
Hy	5.27	3.66	3.71	7.98	3.55	8.86	6.00	6.51	6.98	8.63
Ol	nd	nd	nd	nd	nd	nd	nd	nd	1.76	nd
Ne	nd	nd	nd	nd	nd	nd	nd	nd	nd	nd
C	1.24	1.08	.67478	nd	2.62	nd	.48077	.81986	nd	nd
Q	28.42	35.04	25.24	6.75	30.95	.43581	22.88	6.14	nd	11.29
Tot	99.51	99.93	99.82	99.81	99.89	99.57	99.72	99.73	99.68	99.42
A	51.61	60.39	61.44	41.00	63.75	33.55	49.28	45.67	42.68	36.18
M	10.55	12.60	8.28	13.03	9.98	13.58	12.89	10.63	14.32	19.85
F	37.84	27.00	30.28	45.97	26.27	52.87	37.82	43.70	43.00	43.97
Q	178	207	154	74.85	185	47.88	150	63.52	36.98	101.26
P	-39.85	-134.79	-113.35	-178.48	-38.74	-207.36	-82.12	-179.78	-213.31	-171.93

	MR176	BA10	BA12	BA16	BA18	BA43	BB2	BB3	BB5	BB7
SIO2	70.39	55.43	68.23	69.19	50.75	61.71	64.43	51.37	46.92	57.23
TIO2	0.31	0.31	0.23	0.36	0.83	0.39	0.32	0.73	0.91	0.48
AL203	14.61	20.79	14.70	15.09	18.76	18.51	17.21	22.12	24.01	18.46
FE203	0.17	0.32	0.25	0.21	0.64	0.22	0.21	0.41	0.45	0.36
FEO	1.92	3.59	2.73	2.39	7.14	2.50	2.31	4.53	4.99	3.96
MNO	0.06	0.06	0.02	0.02	0.12	0.06	0.03	0.08	0.09	0.06
MGO	1.30	2.54	1.68	0.89	3.80	1.43	1.64	2.37	2.54	3.62
CAO	2.00	2.61	2.04	1.80	6.46	3.23	2.68	5.49	8.01	4.37
NA20	7.06	10.32	8.95	4.31	8.07	6.72	7.02	9.45	10.06	8.79
K20	2.14	3.93	1.10	5.66	3.17	5.11	4.03	3.24	1.62	2.49
H20+	nd	nd	nd	nd	nd	nd	nd	nd	nd	nd
H20-	nd	nd	nd	nd	nd	nd	nd	nd	nd	nd
P205	0.04	0.11	0.06	0.08	0.26	0.12	0.11	0.23	0.41	0.18
TOTAL	100.00	100.00	100.00	100.00	100.00	100.00	100.00	100.00	100.00	100.00
Ap	.11318	.35079	.18367	.22684	.61092	.34229	.31925	.66479	1.17	.53969
Il	.86191	.95119	.67554	1.04	1.90	1.09	.92751	2.05	2.54	1.44
Mt	.36483	.75540	.54445	.46750	1.13	.47933	.45491	.87680	.95952	.80909
Or	10.88	22.04	5.86	29.54	13.31	26.10	21.12	16.72	8.29	13.55
Ab	33.78	54.59	44.86	21.20	31.94	32.38	34.64	45.94	35.46	45.12
An	9.82	13.62	10.28	8.74	15.81	15.50	13.09	24.33	31.60	19.55
Di	nd	nd	nd	nd	7.84	nd	nd	1.67	4.94	2.23
Hy	3.01	6.58	4.41	2.92	1.98	3.62	3.85	.55634	nd	7.42
Ol	nd	nd	nd	nd	6.64	nd	nd	7.87	8.12	nd
Ne	nd	nd	nd	nd	nd	nd	nd	nd	7.10	nd
C	1.42	1.74	.75879	1.70	nd	.58294	1.12	nd	nd	nd
Q	39.52	2.60	34.61	37.39	nd	18.44	25.74	nd	nd	10.30
Tot	99.77	103.24	102.17	103.22	81.14	98.54	101.26	100.68	100.17	100.95
A	60.89	56.51	53.55	63.88	35.56	63.58	61.89	49.35	43.65	45.74
M	9.99	11.44	11.01	5.70	13.65	8.16	10.04	10.59	11.51	17.15
F	29.12	32.05	35.43	30.42	50.78	28.26	28.07	40.06	44.84	37.11
Q	229	47.32	207	217	20.17	117	157	14.25	-25.33	89.60
P	-122.68	-170.92	-181.02	-8.25	-166.79	-85.86	-102.89	-215.37	-302.47	-195.94

	BB9	al1	al5	al6	ba13	ba14	ba20	ba22	ba23	ba24
SIO2	64.25	57.59	57.46	78.12	60.00	48.71	50.88	48.14	47.41	53.24
TIO2	0.30	0.51	0.45	0.29	0.45	0.89	0.58	0.82	1.05	0.57
AL203	17.44	18.70	19.84	9.68	18.55	20.20	23.91	21.19	23.95	20.65
FE203	0.13	0.33	0.32	0.35	0.31	0.66	0.29	0.60	0.43	0.45
FEO	1.39	3.66	3.52	3.94	3.43	7.32	3.22	6.66	4.79	5.00
MNO	0.02	0.06	0.07	0.03	0.07	0.12	0.09	0.13	0.08	0.08
MGO	1.07	2.99	1.55	1.20	1.65	4.34	1.51	4.24	3.05	2.40
CAO	2.55	3.91	3.51	1.47	3.23	6.25	4.29	6.16	5.59	4.75
NA2O	11.29	8.42	8.72	2.91	8.10	9.15	10.44	9.27	10.58	8.70
K2O	1.47	3.67	4.42	1.78	4.05	2.01	4.51	2.43	2.66	3.95
H2O+	nd	nd	nd	nd	nd	nd	nd	nd	nd	nd
H2O-	nd	nd	nd	nd	nd	nd	nd	nd	nd	nd
P2O5	0.09	0.16	0.15	0.22	0.16	0.35	0.27	0.35	0.41	0.22
TOTAL	100.00	100.00	100.00	100.00	100.00	100.00	100.00	100.00	100.00	100.00
Ap	.26934	.48924	.46301	.62615	.48569	.99125	.77180	1.01	1.18	.66132
Il	.87408	1.51	1.30	.80277	1.30	2.48	1.62	2.30	2.92	1.72
Mt	.27577	.73714	.70649	.75522	.68443	1.40	.62052	1.28	.91739	1.03
Or	7.77	19.70	23.62	9.09	21.55	10.23	23.15	12.40	13.55	21.63
Ab	56.11	42.65	43.98	14.00	40.56	41.93	41.50	38.29	37.82	44.87
An	12.33	17.77	17.42	5.62	15.72	23.02	19.74	24.25	25.03	21.89
Di	.27572	1.50	nd	nd	nd	4.86	nd	3.51	nd	1.75
Hy	2.27	6.38	4.84	4.68	4.85	nd	nd	nd	nd	6.90
Ol	nd	nd	nd	nd	nd	14.39	6.21	14.02	10.38	nd
Ne	nd	nd	nd	nd	nd	1.06	4.85	3.45	7.08	nd
C	nd	nd	.18288	2.61	.47731	nd	1.20	nd	.85160	nd
Q	21.79	9.72	8.09	63.01	15.03	nd	nd	nd	nd	.26884
Tot	101.97	100.46	100.60	101.19	100.66	100.35	99.67	100.50	99.72	100.71
A	73.10	51.25	58.21	32.41	56.48	33.24	62.75	36.38	47.26	47.90
M	7.51	14.26	7.59	8.99	8.51	15.39	7.13	15.48	12.82	10.15
F	19.40	34.49	34.20	58.60	35.01	51.37	30.13	48.15	39.91	41.95
Q	129	82.17	67.04	354	103.48	16.62	-15.65	4.37	-21.40	35.36
P	-229.79	-158.05	-142.92	-45.16	-132.14	-244.72	-187.98	-239.02	-248.64	-174.03

	ba25	ba26	ba27	ba28	ba40	ba41	ba42	ba44	ba45	ba46
SIO2	48.17	74.12	55.96	46.37	52.75	53.45	55.75	59.74	53.67	49.73
TIO2	0.73	0.29	0.64	0.75	0.93	0.56	0.55	0.47	0.68	0.78
AL203	24.29	13.20	18.81	18.45	20.92	19.30	19.83	18.12	19.64	22.39
FE203	0.53	0.11	0.47	0.71	0.44	0.39	0.39	0.35	0.51	0.65
FEO	5.92	1.26	5.25	7.86	4.84	4.37	4.38	3.88	5.69	7.19
MNO	0.10	0.02	0.11	0.11	0.05	0.06	0.07	0.10	0.09	0.12
MGO	2.48	0.39	3.20	11.21	2.20	4.52	2.45	2.05	2.91	2.68
CAO	7.63	1.29	5.24	7.92	3.39	5.22	4.31	2.56	4.73	6.35
NA2O	8.57	5.36	8.24	5.22	7.89	9.35	8.29	8.44	8.31	7.03
K2O	1.31	3.94	1.84	1.11	6.26	2.56	3.79	4.20	3.56	2.84
H2O+	nd	nd	nd	nd	nd	nd	nd	nd	nd	nd
H2O-	nd	nd	nd	nd	nd	nd	nd	nd	nd	nd
P2O5	0.28	0.02	0.23	0.30	0.33	0.21	0.19	0.08	0.22	0.25
TOTAL	100.00	100.00	100.00	100.00	100.00	100.00	100.00	100.00	100.00	100.00
Ap	.80485	.06693	.71324	.90900	.95879	.65930	.58741	.25667	.66809	.77039
Il	2.07	.81084	1.89	2.24	2.67	1.67	1.63	1.39	2.04	2.35
Mt	1.16	.24020	1.07	1.61	.95000	.90056	.88934	.79070	1.18	1.50
Or	6.84	19.95	10.02	6.07	32.73	14.04	20.50	22.81	19.60	15.77
Ab	42.05	25.57	42.33	26.89	38.89	48.36	42.29	43.16	43.13	36.76
An	37.34	6.34	23.81	33.14	14.91	20.27	20.99	13.13	21.41	32.95
Di	nd	nd	2.19	6.34	nd	5.38	.47636	nd	2.17	nd
Hy	.91829	1.32	8.01	9.85	3.44	8.18	6.64	5.90	8.07	8.29
Ol	10.03	nd	nd	14.79	4.14	nd	nd	nd	nd	2.09
Ne	nd	nd	nd	nd	nd	nd	nd	nd	nd	nd
C	.06774	1.30	nd	nd	1.03	nd	nd	.62705	nd	.65115
Q	nd	46.44	10.39	nd	nd	1.13	6.45	13.58	2.47	nd
Tot	101.28	102.03	100.43	101.85	99.73	100.58	100.45	101.65	100.75	101.13
A	36.36	75.11	38.41	16.55	53.15	43.56	49.26	53.92	42.66	34.03
M	11.10	3.33	14.50	34.94	8.76	19.36	11.18	9.70	11.76	10.46
F	52.54	21.56	47.09	48.51	38.09	37.08	39.56	36.38	45.58	55.51
Q	20.08	261	92.11	71.36	21.24	44.70	66.22	102.25	52.45	44.97
P	-274.11	-48.64	-211.11	-223.15	-91.09	-221.29	-160.47	-125.00	-173.00	-192.03

	ba47	ba48	ba50	ba51	ba52	bb15	bb16	bb17	bb18	MT15
SIO2	63.54	66.56	56.37	61.29	55.81	53.02	55.09	64.32	57.68	72.39
TIO2	0.35	0.37	0.54	0.43	0.60	0.64	0.56	0.51	0.63	0.29
AL2O3	17.34	14.97	19.46	17.60	19.10	19.93	19.45	16.13	18.11	14.00
FE2O3	0.31	0.41	0.38	0.37	0.42	0.46	0.38	0.17	0.51	0.20
FEO	3.42	4.56	4.26	4.16	4.72	5.14	4.24	1.88	5.70	2.23
MNO	0.10	0.08	0.07	0.06	0.08	0.10	0.05	0.02	0.08	0.02
MGO	1.27	1.12	2.35	2.22	2.80	3.00	2.77	1.24	3.46	0.50
CAO	1.92	1.99	4.06	2.55	4.42	4.59	4.25	3.13	3.18	2.63
NA2O	7.69	4.79	8.22	7.24	8.28	9.54	9.35	11.20	7.08	5.99
K2O	3.94	5.06	4.06	3.97	3.54	3.33	3.65	1.26	3.42	1.72
H2O+	nd	nd	nd	nd	nd	nd	nd	nd	nd	nd
H2O-	nd	nd	nd	nd	nd	nd	nd	nd	nd	nd
P2O5	0.12	0.08	0.22	0.10	0.23	0.25	0.21	0.15	0.14	0.04
TOTAL	100.00	100.00	100.00	100.00	100.00	100.00	100.00	100.00	100.00	100.00
Ap	.34654	.23392	.65650	.30465	.70720	.77023	.63049	.42378	.43334	.11299
Il	1.02	1.07	1.60	1.26	1.77	1.90	1.66	1.43	1.90	.82134
Mt	.67909	.90701	.86576	.83591	.96388	1.04	.86380	.36244	1.18	.42691
Or	20.84	26.82	21.97	21.27	19.24	18.05	19.81	6.47	18.81	8.80
Ab	38.38	23.93	41.93	36.59	42.43	48.65	47.78	54.30	36.66	28.85
An	9.13	9.86	19.43	12.78	19.79	19.09	17.49	9.43	16.19	13.12
Di	nd	nd	.50443	nd	1.76	2.86	3.07	4.52	nd	nd
Hy	4.47	5.28	6.40	6.29	7.09	5.96	6.26	1.60	9.36	2.30
Ol	nd	nd	nd	nd	nd	2.13	nd	nd	nd	nd
Ne	nd	nd	nd	nd	nd	nd	nd	nd	nd	nd
C	2.20	1.36	nd	1.59	nd	nd	nd	nd	1.73	1.08
Q	23.93	32.16	7.36	19.78	6.94	nd	3.11	21.87	14.18	46.15
Tot	101.00	101.62	100.73	100.71	100.70	100.46	100.67	100.39	100.45	101.66
A	56.66	48.59	50.62	49.40	46.34	46.00	50.62	67.04	39.00	57.41
M	6.86	5.68	10.76	10.76	12.37	12.30	12.24	8.23	14.31	4.33
F	36.48	45.73	38.63	39.84	41.29	41.70	37.15	24.73	46.69	38.25
Q	150	197	69.39	136	70.09	31.91	46.44	126	119	262
P	-102.83	-30.84	-150.13	-105.43	-167.07	-197.92	-182.68	-238.39	-123.42	-123.42

	MT18	MT19	MT22	MT23	MU1	MU10	MU11	MU2	MU3	MU4
SIO2	68.92	59.81	59.10	63.19	63.78	66.73	60.87	58.07	55.88	55.43
TIO2	0.35	0.22	0.23	0.35	0.35	0.15	0.58	0.48	0.67	0.61
AL203	15.08	20.23	17.08	17.60	16.98	16.93	18.06	18.47	21.84	19.08
FE203	0.21	0.21	0.65	0.22	0.26	0.17	0.28	0.35	0.40	0.43
FEO	2.29	2.31	7.19	2.42	2.93	1.85	3.15	3.90	4.39	4.78
MNO	0.04	0.04	0.08	0.04	0.05	0.02	0.05	0.06	0.07	0.08
MGO	0.85	0.87	4.01	1.76	1.54	1.08	1.80	3.21	2.73	3.02
CAO	1.67	4.26	4.58	2.86	2.75	3.17	2.91	4.27	2.65	4.58
NA20	6.07	10.86	5.47	7.84	6.91	8.44	7.19	7.36	10.71	8.50
K20	4.47	1.10	1.55	3.61	4.34	1.42	4.90	3.65	0.40	3.27
H20+	nd	nd	nd	nd	nd	nd	nd	nd	nd	nd
H20-	nd	nd	nd	nd	nd	nd	nd	nd	nd	nd
P205	0.06	0.09	0.06	0.12	0.12	0.05	0.22	0.16	0.26	0.23
TOTAL	100.00	100.00	100.00	100.00	100.00	100.00	100.00	100.00	100.00	100.00
Ap	.18130	.27294	.19839	.34277	.34458	.13582	.64415	.49205	.77669	.70759
Il	1.00	.62986	.70821	1.01	1.01	.43097	1.67	1.42	1.93	1.82
Mt	.44311	.46124	1.51	.48152	.58573	.36484	.62457	.79089	.86596	.98154
Or	23.06	5.86	8.66	19.14	23.13	7.48	25.94	19.75	2.09	17.86
Ab	29.55	54.50	28.80	39.20	34.72	41.87	35.83	37.49	53.04	43.81
An	8.10	21.86	25.02	14.18	13.64	16.29	13.49	20.16	11.60	20.01
Di	nd	nd	nd	nd	nd	nd	nd	1.23	nd	2.43
Hy	2.78	3.04	12.07	4.12	4.34	2.90	4.62	7.03	6.80	7.29
Ol	nd	nd	nd	nd	nd	nd	nd	nd	nd	nd
Ne	nd	nd	nd	nd	nd	nd	nd	nd	nd	nd
C	1.33	.05492	1.14	.79172	.60579	.84883	.83938	nd	6.09	nd
Q	35.12	14.74	22.21	22.66	24.07	32.15	17.41	12.60	13.44	6.18
Tot	101.56	101.42	100.32	101.93	102.45	102.47	101.08	100.96	96.63	101.09
A	64.75	63.90	24.78	61.01	58.58	63.24	58.36	47.59	43.23	45.32
M	5.59	5.78	16.52	10.46	8.70	8.38	9.34	15.39	13.55	13.21
F	29.66	30.32	58.70	28.53	32.72	28.39	32.31	37.02	43.23	41.47
Q	204	94.99	172	142	150	189	114	100.23	101.61	67.05
P	-59.06	-259.47	-151.52	-130.28	-97.66	-187.41	-94.47	-145.49	-228.81	-179.97

	MU5	MU6	MU7	a14	ba15	ba49	mt24	CH4	CH2	CH3
SIO2	53.39	64.29	56.78	56.99	67.74	60.85	64.90	53.63	53.95	53.57
TIO2	0.70	0.49	0.60	0.41	0.23	0.88	0.84	0.66	0.56	0.55
AL2O3	20.09	16.07	18.76	20.53	16.25	16.50	17.35	19.04	19.30	19.77
FE2O3	0.45	0.32	0.47	0.24	0.16	0.53	0.19	0.57	0.47	0.55
FEO	5.01	3.60	5.22	2.62	1.75	5.85	2.16	6.29	5.27	6.07
MNO	0.08	0.04	0.09	0.07	0.04	0.08	0.01	0.12	0.08	0.10
MGO	3.53	2.55	2.56	1.01	0.68	2.50	1.21	3.03	3.84	3.65
CAO	4.72	2.90	4.52	2.47	1.76	3.43	2.61	5.90	5.33	5.32
NA2O	8.87	5.84	7.38	9.60	5.17	4.97	6.51	8.50	8.80	7.42
K2O	2.88	3.78	3.40	5.93	6.18	4.04	4.20	2.04	2.13	2.81
H2O+	nd	nd	nd	nd	nd	nd	nd	nd	nd	nd
H2O-	nd	nd	nd	nd	nd	nd	nd	nd	nd	nd
P2O5	0.30	0.11	0.21	0.14	0.05	0.37	0.01	0.22	0.26	0.19
TOTAL	100.00	100.00	100.00	100.00	100.00	100.00	100.00	100.00	100.00	100.00
Ap	.93008	.32579	.64110	.41063	.15768	1.12	.04501	.66866	.78718	.58124
Il	2.11	1.39	1.79	1.20	.64330	2.62	2.63	1.96	1.67	1.66
Mt	1.04	.70864	1.06	.52893	.34223	1.19	.46381	1.28	1.07	1.25
Or	15.88	19.81	18.49	31.91	32.18	21.96	24.05	11.09	11.59	15.48
Ab	46.13	28.82	37.81	48.72	25.36	25.48	35.14	43.53	45.04	38.47
An	23.01	14.25	21.71	12.05	8.68	15.33	14.79	23.13	22.73	26.19
Di	.20946	nd	.79437	nd	nd	nd	nd	5.72	3.22	1.12
Hy	8.70	6.00	7.49	3.38	2.22	7.91	2.91	7.86	8.61	9.78
Ol	nd	nd	nd	nd	nd	nd	nd	nd	nd	nd
Ne	nd	nd	nd	nd	nd	nd	nd	nd	nd	nd
C	nd	.97861	nd	.51340	1.49	1.85	1.55	nd	nd	nd
Q	2.46	27.69	10.86	3.19	31.70	24.57	31.15	4.38	4.31	4.85
Tot	100.47	99.97	100.64	101.92	102.77	102.04	113	99.64	99.04	99.37
A	43.11	47.89	42.78	69.80	72.98	37.74	64.39	36.52	39.32	36.47
M	14.92	13.71	11.36	4.91	4.40	11.04	7.85	12.42	16.33	14.79
F	41.97	38.40	45.85	25.29	22.62	51.21	27.77	51.06	44.35	48.74
Q	53.06	176	92.93	33.96	184	162	185	61.25	62.96	72.99
P	-195.96	-88.31	-153.87	-114.58	-13.59	-78.69	-98.93	-222.50	-215.95	-178.32